Volume 7 JULY, 1936 Number 7

PHYSICS

A Journal of General and Applied Physics

The Piezoelectric Resonator and the Effect of Electrode Spacing upon Frequency

WALTER G. CADY, *Wesleyan University*

(Received May 1, 1936)

A new formulation of piezo-resonator theory, called for convenience the "*mechanical theory*," is developed for a crystal resonator with gap between crystal and electrodes, involving the increase in effective stiffness caused by space or surface charge, and explaining the increase in resonance frequency with increasing gap. The cases treated are thickness vibrations (both compressional and shear) of a plate, and lengthwise compressional vibrations of a bar. Specialized values of the elastic, dielectric and piezoelectric constants are employed, depending upon the nature of the elastic reactions for each cut and for each mode of vibration. The mechanical theory is compared with the customary "*electrical theory*," according to which the resonator maintains a constant stiffness, the increase in frequency with increasing gap being accounted for by the electrical reactance of the gap considered as a series capacitance. When the crystal surfaces are equipotential (thickness vibrations, or lengthwise vibrations of a bar whose surfaces have been covered with a metallic deposit), the two theories are in agreement. It is shown that the mechanical theory, unlike the electrical theory, describes correctly the performance of a vibrating crystal bar that is not metallically coated. The characteristics of the resonator and the contrast between the two theories are illustrated by resonance-circle and phase diagrams. The *relative increase in frequency* caused by the gap is shown to be $\Delta f/f_0 = Uw/(e+kw)$, where f_0 is the frequency at zero gap, $f_0+\Delta f$ the frequency with a gap of width w, e the thickness of the crystal in the direction of the applied electric field, k the dielectric constant and $U=16\epsilon^2/\pi c$, ϵ being the appropriate piezoelectric constant and c the effective elastic constant at zero gap. In the case of the uncoated bar, the function U has to be multiplied by $\pi^2/8$. *Observations* were made with eight *quartz crystals* of the following cuts: Y-cut, X-cut, BT- and AC-cuts (notation of Lack, Willard and Fair) for thickness vibrations, and an X-cut bar for lengthwise vibrations. With small gaps, the experimental values of the function U are, except with the BT- and AC-cuts, from 13 to 60 percent smaller than the theoretical values. In most cases the discrepancy becomes still greater at large gap values. The probable reasons for these discrepancies are discussed, with the conclusion that a large increase in frequency with gap may be taken as a criterion of a good resonator (large piezoelectric constant, freedom from twinning and coupling). A *Rochelle salt* Y-cut 45° bar when tested for the gap effect showed a satisfactory agreement with theory, considering the uncertainty in the values of the dielectric and piezoelectric constants. It is shown that the effect of gap upon frequency can be utilized in determining approximately the piezoelectric constant of a crystal. The theory of the dependence of frequency upon gap for *overtone* vibrations is briefly discussed.

INTRODUCTION

PIEZOELECTRIC resonators are frequently provided with a free space between the crystal and one or both electrodes, although there is a growing practice of using as electrodes thin metallic films deposited directly on the crystal surfaces. When present, the gaps modify the over-all mechanical and electrical constants of the resonator; they thus affect both amplitude and natural frequency of vibration. The gap effect is dependent on space and surface charge phenomena associated with the cut and mode of vibration employed. It yields to simple theoretical treatment only in the cases of relatively thin plates and of relatively long rods. Even with this simplification, a rigorous theory of the resonator, with or without a gap, would have to take account of boundary conditions, all elastic, frictional and electric constants of the material, coupling effects between vibrations of various modes, nonuniformity of applied electric field and, when air gaps are present, resonance effects

in the air itself. Solutions of special problems involving certain of these considerations have been offered by many writers.

The present paper is restricted to thickness vibrations of plates and lengthwise vibrations of bars, modes which are of both scientific and engineering interest. The present treatment differs from previous discussions chiefly in offering a more complete explanation of the influence of the gap upon the effective stiffness of the crystal. It is assumed that only one degree of freedom need be considered; that the impressed electric field remains uniform even with the largest gaps; and that frictional and resonance effects due to air in the gap may be ignored. The discrepancies which these idealized conditions introduce between theory and observation will be discussed in §19.

I. Theory of the Resonator

The electrical theory

§1. It has become customary to consider the crystal as equivalent to a pure dielectric capacitance C_1, Fig. 1a, in parallel with the series chain RLC.[1, 2] When a gap is present, it is treated as a series capacitance C_2.[2, 3] R, L, C and C_1 are regarded as fixed constants for each particular resonator, as are also the mechanical constants of the crystal. We shall for convenience refer to this theory as the "electrical theory," in contrast to the "mechanical theory" which is about to be developed. Watanabe[3] has shown that for the network in Fig. 1a can be substituted, at all frequencies, that shown in Fig. 1b, where

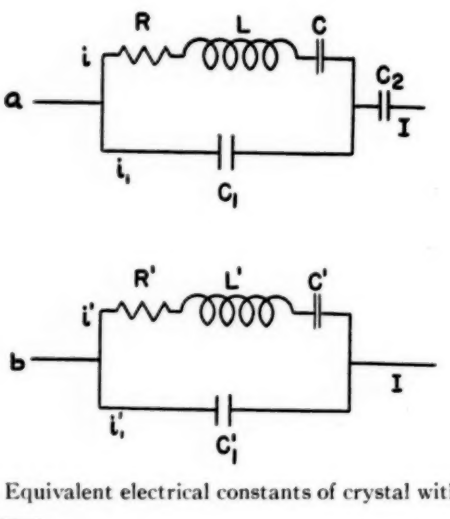

Fig. 1. Equivalent electrical constants of crystal with gap.

$$R'/R = L'/L = (1 + C_1/C_2)^2, \tag{1}$$

$$\frac{C}{C'} = \left(1 + \frac{C_1}{C_2}\right)\frac{C + C_1 + C_2}{C_2} = \left(1 + \frac{C_1}{C_2}\right)^2 + \frac{C}{C_2}\left(1 + \frac{C_1}{C_2}\right), \tag{2}$$

$$C_1/C_1' = 1 + C_1/C_2. \tag{3}$$

R, L, C and C_1 are the equivalent electrical constants for the crystal with zero gap, while C_2 is the capacitance of the gap. Equivalent networks of substantially the same type had previously been treated by Johnson and Shea.[4] Although the equivalent electrical constants have frequently been measured, few writers have paid any attention to the effect of the piezoelectric polarization field on the elastic constant, and none, so far as is known to the writer, has considered the effect of the gap on this quantity. It has been customary to treat the elastic constant as a fixed quantity, unaffected by the gap.

It is already known that space and surface charges caused by polarization of the crystal may have effects on the resonator constants,[5–10] but hitherto this consideration has been applied only to a few special cases, in none of which has the universal validity of Eqs. (1) and (2) been questioned. In the present paper these effects are treated more rigorously and with greater generality, in order to see under what circumstances Eqs. (1) and (2) hold. Thickness vibrations of thin plates, of compressional and shear modes, as well as longitudinal vibrations of bars, are con-

[1] K. S. Van Dyke, Phys. Rev. **25**, 895 (1925); Proc. I. R. E. **16**, 742 (1928).
[2] D. W. Dye, Proc. Phys. Soc. London **38**, 399 (1926).
[3] Y. Watanabe, Elec. Nach. Tech. **5**, 45 (1928); Proc. I. R. E. **18**, 695 (1930).
[4] K. S. Johnson and T. E. Shea, Bell Sys. Tech. J. **4**, 52 (1925).
[5] E. Giebe and A. Scheibe, Ann. d. Physik **9**, 93 (1931).
[6] I. Koga, Physics **3**, 70 (1932).
[7] J. Kobzarew, J. Appl. Phys. (Moscow) **6**, 17 (1929).
[8] M. v. Laue, Zeits. f. Physik **34**, 347 (1925).
[9] E. Giebe and A. Scheibe, Zeits. f. Physik **46**, 607 (1928).
[10] I. Koga, Rep. Rad. Res. and Works in Japan **2**, 157 (1932).

sidered. Application is made to several well-known cuts in quartz, and the results are compared with experimental data.

The mechanical theory

(*a*) *Thickness vibrations*

§2. *The generalized theory for thin plates* will be developed first, applicable to all crystals and all cuts which satisfy the requirement that an alternating electric field normal to the surface of the plate causes vibrations (compressional or shear) with wave propagation parallel to the field. For convenience, this normal direction will here be denoted by x, and elastic strains, whether of compressional or shear type, by x_x; when application is made to particular cuts, the axial direction appropriate to each cut will be substituted (Table I). Strictly, the theory is applicable only to plates of infinite area, in which case the only strain is that characteristic of the thickness vibration. If the boundaries are finite, then as is well known various other vibration modes may become excited, due not only to primary piezoelectric effects but to various elastic reactions (coupling effects) as well. These other modes may be expected to complicate the electric conditions in the crystal, and thus to modify the conclusions derived from the present theory, as will be discussed in §19. It would be extremely difficult to include these disturbing effects in the theory, and perhaps even more difficult to test so complete a theory experimentally. In any case, even if coupling effects were taken into account, failure of experimental results to conform very exactly to theory must be expected, owing, even when great care is expended, to such unavoidable causes as nonuniformity of electric field, nonparallelism of crystal and electrode surfaces, imperfect orientation of crystal plate, mechanical defects in the crystal, and especially, when adjustable electrodes are used, the impossibility of taking readings with the gap at strictly zero value.

The resonator is a plate of piezoelectric crystal of thickness e, between conducting electrodes, as shown in Fig. 2. The surface area is assumed to be so great that boundary effects can be ignored. The total gap is w; under our simplifying assumptions it does not matter whether the gap is all on the same side of the crystal or not. The possible effect of the position of the crystal between the electrodes on the frequency, for a finite plate, is discussed in §20. The instantaneous driving voltage impressed on the electrodes is $V=V_0\cos\omega t$, and hence the driving voltage across the crystal is

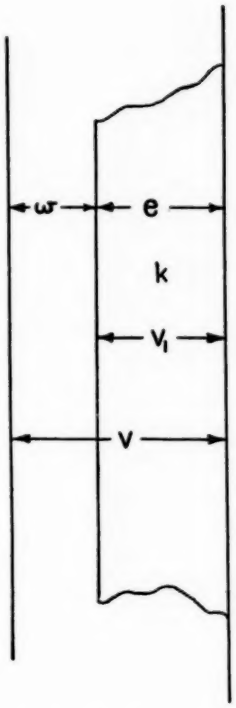

FIG. 2. Resonator for thickness vibrations.

$$V_1=eV/e', \tag{4}$$

where $e'=e+kw$. For k we take the value of the dielectric constant appropriate to the orientation of the particular crystal cut used. (As a matter of dimensional consistency it should be said that k is here strictly the ratio of the dielectric constant of the crystal to that of the gap.) V_1 causes in the crystal an instantaneous driving field $E_1=V_1/e=V/e'$. The corresponding field in the gap is

$$E_w=kE_1. \tag{5}$$

Since we are dealing with a one-dimensional problem and are confining ourselves to the resonance region for the fundamental thickness frequency, we may substitute for the crystal an equivalent mechanical system of concentrated mass M, frictional resistance W, and stiffness

including effect of gap G'. This method was first used for lengthwise vibrations[11, 12] and has now become common practice. The equation of motion, for the resonance region, is

$$M\frac{d^2\xi}{dt^2}+W\frac{d\xi}{dt}+G'\xi=F_0\cos\omega t, \tag{6}$$

where ξ is the equivalent mechanical displacement, equal to the actual displacement of either face of the crystal, the nodal plane being at rest.

A word should be said at this point concerning *shear vibrations* in y-cut quartz plates. The same considerations apply equally to all types of vibration in which the axis of shear lies in the plane of the plate, and this includes the AC and BT cuts treated in §8. For the y-cut quartz resonator the stress and strain are X_y and x_y, respectively, and the direction of ξ lies in the plane of the plate, instead of being normal to the surface as in the X-cut. In the neighborhood of resonance the distribution of strain is sinusoidal, exactly as with compressional waves. The equivalent mass M is the same, as may be proved by consideration of kinetic energy. X in Eq. (8) means in this case a tangential stress X_y. All the resonator equations here given, and hence the equivalent electrical networks, are applicable equally to shear and compressional modes. Numerical values vary, of course, from one type to another, as shown in Table I.

As in the case of a longitudinally vibrating rod,[11] the equivalent instantaneous sinusoidal impressed force (positive when extensional), is

$$F=F_0\cos\omega t=-2AX=2\epsilon AE_1$$
$$=2\epsilon AV/e'=(2\epsilon AV_0/e')\cos\omega t, \tag{7}$$

where X is the instantaneous driving mechanical stress for thickness vibrations, given by the equation

$$X=-\epsilon E_1 \tag{8}$$

in which ϵ is the piezoelectric constant relating E_1 to X.

According to Voigt's terminology, which is here followed, a stress is positive when compressional, while a strain is positive when extensional. This, together with the assumption that the driving force F is positive when compressional, accounts for the negative signs in Eqs. (7) and (8).

On solving (6) and substituting from (7) we have for the maximum displacement (using primed quantities for the general case where a gap is present)

$$\xi_0=\frac{F_0}{\omega Z_c}=\frac{2\epsilon AV_0}{\omega e'Z_c'}=\frac{2\epsilon AV_0}{\omega e'}Y_c'. \tag{9}$$

The mechanical impedance of the crystal is given by

$$Z_c'^2=W^2+(\omega M-G'/\omega)^2. \tag{10}$$

$Y_c'=1/Z_c'$ represents the mechanical admittance. The displacement at time t is

$$\xi=\xi_0\sin(\omega t-\theta), \tag{11}$$

where
$$\tan\theta=(\omega M-G'/\omega)/W. \tag{12}$$

For the velocity of motion at the surface of the crystal we find from Eq. (11)

$$v=d\xi/dt=\omega\xi_0\cos(\omega t-\theta). \tag{13}$$

From Eq. (9) it is clear that v is a maximum at that frequency for which Z_c is a minimum, the mechanical reactance being then zero.

The equivalent mechanical constants, for a plate of large area A, are found, by the same method as for lengthwise vibrations,[9] to be

$$M=\rho eA/2,\ W=\pi^2\rho QA/2e,\ G'=\pi^2c'A/2e, \tag{14}$$

where ρ and Q are the crystal density and viscosity, and c' the effective elastic constant derived in §4. As will be seen, G' and c' themselves are functions of the gap. The equation for G' is derived from that for M together with the resonance relation $M\omega=G'/\omega$ and the fact that for the fundamental vibration frequency $(c'/\rho)^{\frac{1}{2}}=2fe$. In actual resonators, W usually depends chiefly on the mounting and surrounding air. The true quartz viscosity Q is very small; no reliable values for thickness vibrations seem to have been published. Van Dyke[13] finds for an X-cut Y-wave quartz bar vibrating lengthwise in vacuum a value of the "internal friction

[11] W. G. Cady, Proc. I. R. E. **10**, 83 (1922).
[12] W. G. Cady, Phys. Rev. **19**, 1 (1922).
[13] K. S. Van Dyke, Proc. I. R. E. **23**, 386 (1935).

constant" (ratio of logarithmic decrement to Young's modulus) equal to 7 (10^{-18}), whence from the equations in §6 the value of Q is 1.1. If the decrement of the resonator is measured, the over-all value of W may be found from the equation $\Delta = W/2fM$, f being the resonance frequency and Δ the logarithmic decrement.

In order to deduce the equivalent electrical constants, we seek an equation for the instantaneous current I flowing to the resonator. This is of two components (Fig. 1):

$$I = i_1' + i' = C_1' dV/dt + (A/4\pi)(dD/dt). \quad (15)$$

C_1' represents the pure dielectric, or "geometrical," capacitance of crystal and gap together, including the stray capacitance of mounting and leads. It is an important parameter and should preferably be measured directly for each gap whenever the theory is applied to experimental results. Theoretically, ignoring stray capacitance and assuming the crystal surfaces to be equipotential, C_1' is the capacitance of two condensers $C_1 = kA/4\pi e$ and $C_2 = A/4\pi w$ in series (Fig. 1), so that $C_1' = kA/4\pi e' = C_1C_2/(C_1+C_2)$, as in Eq. (3). C_1 had best be measured rather than calculated. Unless the gap is relatively large, the above equation for C_2 can safely be assumed to be approximately correct, and this assumption is made throughout (see Sec. 19).[14]

§3. *Equivalent electrical constants.* The second component of current, i, in Eq. (15), which may be called the piezo-current, owes its existence to the piezoelectric displacement D. This quantity is derived as follows. We assume that the strain distribution in the crystal is sinusoidal in both space and time, and that at any given time t the equation for the instantaneous strain at distance x from the central, or nodal, plane of the crystal (for frequencies in the neighborhood of the fundamental) is

$$x_x = x_{x0} \cos(\pi x/e)$$

where x_{x0} is the strain at the center. The origin, as shown in Fig. 3, is at the center of the plate AB. The gap is $w = A'A + BB'$. The curve for x_x is not shown, but it would be similar to the curve P.

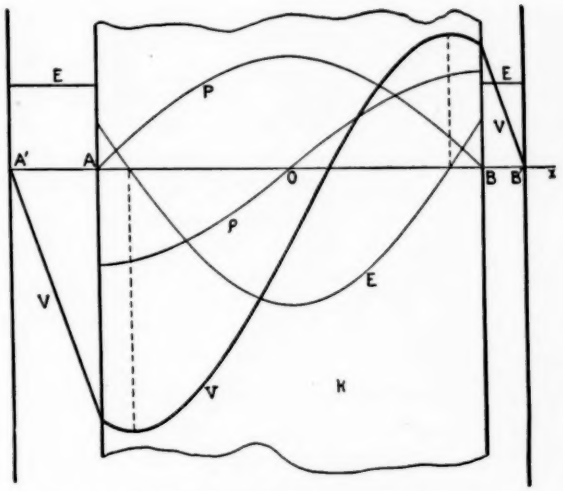

FIG. 3. Distribution of polarization P, space charge ρ, electric intensity E and potential V, in a resonator for thickness vibrations. Crystal thickness AB $= e$.

In order to establish a relationship with Eq. (9) and thence to find the equivalent electrical constants, it is desirable to express D in terms of ξ, the instantaneous mechanical displacement at point B in Fig. 2, at which $x = e/2$. It is easily verified that $x_{x0} = \pi\xi/e$, whence

$$x_x = (\pi\xi/e) \cos(\pi x/e). \quad (16)$$

At any x the piezoelectric polarization is

$$P(x) = \epsilon x_x = \frac{\pi\epsilon\xi}{e} \cos\frac{\pi x}{e} = P_0 \cos\frac{\pi x}{e}, \quad (17)$$

where $P_0 = \pi\epsilon\xi/e$. This gives rise to a space charge

$$\rho(x) = -\frac{dP(x)}{dx} = \frac{\pi P_0}{e} \sin\frac{\pi x}{e} = \rho_0 \sin\frac{\pi x}{e}, \quad (18)$$

where $\rho_0 = \pi P_0/e = \pi^2\epsilon\xi/e^2$.

The space charge causes a component of electric intensity E shown in Fig. 3, the value

[14] In the author's original paper, reference 11, that portion of the deformation of the crystal that would have been produced by a static potential difference V was referred to as the "equilibrium elongation." This complication is now avoided by taking for the dielectric constant a value based upon the constraints that characterize the particular type of vibration (§10). Coupled modes are here ignored. A further departure from the original paper lies in defining the electric displacement in the dielectric as $D = kE$, in conformity with modern usage, instead of $D = kE/4\pi$.

of which at any x in the crystal has been derived in a former paper:[15]

$$E(x)=\frac{4\rho_0 e}{k}\left(\frac{2e}{\pi e'}-\cos\frac{\pi x}{e}\right)$$

$$=\frac{4\pi^2\epsilon\xi}{ke}\left(\frac{2e}{\pi e'}-\cos\frac{\pi x}{e}\right). \quad (19)$$

The second term in Eq. (19) is that which results from writing $E(x)=-4\pi P(x)/k$ directly. Koga[6, 10] derives an expression equivalent to this, but he does not consider the first term, which depends on the *distribution* of P and expresses the gap effect. The curve V in Fig. 3 represents the potential distribution in crystal and gaps, on the assumption that the electrodes are at zero potential. The potential equation is given in reference 15, but it is not needed in the present paper.

The total field at any point x in the crystal has two components, $E(x)$ due to the strain, and the impressed field $E_1=V/e'$ from Eq. (1). By deriving $E(x)$ on the assumption of zero potential difference between electrodes we have separated the two components. E_1 accounts for the first term in Eq. (15) and has nothing to do with the piezoelectric reactions. The second term in Eq. (15) is derived from $E(x)$, as will now be proved.

By setting $x=\pm e/2$ in Eq. (19) we find for the electric intensity in the gap due to the strain, and therefore for the corresponding displacement component,

$$E_w=D=8\pi\epsilon\xi/e'. \quad (20)$$

It may be noted that the displacement D, which by the principle of continuity is the same throughout the resonator, depends entirely on the value of E at the crystal surfaces. The effect of the *form* of the E curve on the mechanical stiffness will be discussed in §4.

From Eqs. (7), (15) and (20) the resonator current is

$$I=i_1'+i'=\frac{kA}{4\pi e'}\frac{dV}{dt}+\frac{2\epsilon A}{e'}\frac{d\xi}{dt}=$$

$$-\frac{k\omega A V_0}{4\pi e'}\sin\omega t+\frac{4\epsilon^2A^2V_0}{e'^2Z_c}\cos(\omega t-\theta). \quad (21)$$

[15] W. G. Cady, Physics **6**, 10 (1935).

We are concerned at present only with the second term, which represents the piezo-current i flowing through the equivalent electrical impedance denoted by Z'. The maximum current value can thus be expressed as $i_0=V_0/Z'=V_0/\{R'^2+(\omega L'-1/\omega C')^2\}^{\frac{1}{2}}$, where R', L' and C' are the equivalent electrical constants. Comparison of this equation with Eqs. (10) and (21) shows at once that, calling

$$r'=e'^2/4\epsilon^2A^2, \quad (22)$$

$$Z'=r'Z_c,\quad R'=r'W,\quad L'=r'M,\quad C'=1/r'C'. \quad (23)$$

The primes refer to crystal with gap. When there is no gap, r' reduces to $r=e^2/4\epsilon^2A^2$ and Eq. (23) becomes

$$Z=rZ_c,\quad R=rW,\quad L=rM,\quad C=1/rC. \quad (24)$$

These values of R, L and C are in agreement with those first derived by Van Dyke.[1] Just as the crystal without gap has as its equivalent electrical constants the capacitance C_1 in parallel with the series chain R, L, C, so when a gap is present, the equivalent constants consist of C_1' in parallel with R', L', C'. This is evident from Eq. (15) or (21), the two terms of which represent the current in the parallel condenser C_1' and the piezo-current in the $R'L'C'$ chain, respectively.

Comparison of Eq. (23) with (24) shows that the effect of the gap upon the equivalent electrical constants is contained in the electromechanical ratio r', which involves the quantity $e'=e+kw$, w being the gap width; and, moreover, in the case of C', the mechanical stiffness G', when the gap is present, is slightly greater than G for zero gap, as will presently be explained. Consideration of the ratio r' shows that the combination of crystal and gap is electrically equivalent to a crystal of the same dielectric constant with adherent electrodes, of thickness e', having its mechanical resistance and mass increased in the ratio $(e'/e)^2$, and its stiffness increased in a slightly higher ratio.

§4. *Equations for elastic constants.* We turn now to the effect of the gap upon the equivalent stiffness G' and effective elastic constant c', the relation between which was expressed in Eq. (14). Consider the reacting stresses when the crystal surfaces are displaced by an amount ξ at $e/2$, Fig. 3 and $-\xi$ at $-e/2$ (points B and A, respectively). These reacting stresses do not

include the driving stress X of Eq. (7). For a given ξ, we have seen that the strain distribution is given by Eq. (16):

$$x_x=(\pi\xi/e)\cos(\pi x/e)=X_t/c'. \tag{25}$$

In the last member of Eq. (25) the strain at any point is expressed in terms of total stress (exclusive of the driving stress) and effective elastic constant. The chief component of X_t is, of course, the pure elastic stress, which for generality we will call $X_0=-c_0x_x$, c_0 being the pure elastic constant appropriate to the material and orientation of the plate. For example, with an x-cut quartz plate this takes the familiar form $X_x=-c_{11}x_x$. In a non-piezoelectric substance X_0 is the only reacting stress. When the material is piezoelectric and under *uniform* strain in a direction parallel to the field (lengthwise vibrations, §6), then with zero gap X_0 is still the only reacting stress; when a gap is present, there is an additional stress component due to polarization surface charge. With thickness vibrations the strain is sinusoidally distributed, and the resulting space charge, as will be shown, causes two additional stress components X_1 and X_2, the latter of which is dependent on the gap. We now proceed to derive the elastic constants, or, as they may more appropriately be called, the *quasi-elastic* constants, corresponding to these two stress components.

From Eq. (19) and Fig. 3 it is seen that the electric intensity E due to space charge is of sinusoidal form, having negative values in the interior of the crystal and positive near the outer surfaces. The vertical displacement of the curve is expressed by the first term in Eq. (19), which, by the factor e', depends upon the gap. The significance of this becomes evident when we consider the mechanical stresses that E causes in the crystal, through the converse piezoelectric effect, which in generalized form may be written $X=\epsilon E$. On applying this equation to Eq. (19) there results

$$X_2+X_1\cos\frac{\pi x}{e}=\frac{4\pi^2\epsilon^2\xi}{ke}\left(\frac{2e}{\pi e'}-\cos\frac{\pi x}{e}\right), \tag{26}$$

where

$$X_1=-4\pi^2\epsilon^2\xi/ke \quad\text{and}\quad X_2=8\pi\epsilon^2\xi/ke'. \tag{27}$$

It is easily verified that wherever E is positive, the resulting stress has the same sign as the assumed strain x_x; it therefore is opposed to the pure elastic restoring stress and tends to lower the vibration frequency. Where E is negative, as is predominantly the case, the opposite is true.

From Eqs. (16), (26) and (27),

$$X_1=-(4\pi\epsilon^2/k)x_x\equiv-c_1x_x. \tag{28}$$

The stress X_1 at any point is thus seen to be a constant times the strain at the same point, whence it is evident that c_1, the coefficient of x_x, is of the nature of an elastic coefficient that is constant throughout the crystal. This quasi-elastic constant has also been derived for certain special cases by other writers.[5, 6] Together with the constant c_2, it should never be overlooked when elastic constants are computed from thickness vibrations. For example, it offers an explanation of the discrepancy between theory and observation noted by Bechmann.[16] According to Voigt's notation, the negative sign in Eq. (28) indicates that c_1 is to be added to the pure elastic constant c_0.

The case is not so simple with X_2, as it is not a sinusoidal term. It is rather a stress uniform throughout the crystal and is therefore to be treated in a manner analogous to that used for the driving stress X, Eq. (7). Like X_1, X_2 is proportional to and in phase with ξ, and hence is not a part of the driving stress. Nevertheless, it may, like X in Eq. (7), be regarded as a stress applied *at the surfaces* of the resonator. We may therefore regard it, from the point of view of the equivalent mechanical system with concentrated mass M, as supplying a component of the total restoring force G' acting on M when the instantaneous displacement is ξ. As was shown for the case of X in previous papers,[11, 12] we must take $2AX_2$ as this component. We thus obtain the equivalent stiffness component G_2 from Eq. (27):

$$2AX_2=16\pi\epsilon^2A\xi/ke'\equiv-G_2\xi$$

where

$$G_2=-16\pi\epsilon^2A/ke'. \tag{29}$$

The negative sign results from Voigt's convention respecting the definitions of stress and strain.

[16] R. Bechmann, Zeits. f. tech. Physik **16**, 525 (1935).

To G_2 there corresponds the second of the quasi-elastic constants, c_2. The vibration frequency is determined by the three quantities c_0, c_1 and c_2, whose sum is the total effective elastic constant c'. Their relation to the equivalent stiffness G' may be expressed by writing Eq. (14) thus:

$$G'=G_0+G_1+G_2=(\pi^2A/2e)(c_0+c_1+c_2). \quad (30)$$

The chief component of stiffness is G_0, related to the pure elastic constant c_0 by the equation $G_0=\pi^2Ac_0/2e$. From (30) it is seen that $G_2=\pi^2Ac_2/2e$, whence from Eq. (29)

$$c_2=-32\epsilon^2e/\pi ke'. \quad (31)$$

From Eqs. (30) and (31), together with (28), the final form of the effective stiffness G' is found to be

$$G'=G_0+G_1+G_2$$
$$=\frac{\pi^2A}{2e}\left(c_0+\frac{4\pi\epsilon^2}{k}-\frac{32\epsilon^2e}{\pi ke'}\right)=\frac{\pi^2Ac'}{2e}. \quad (32)$$

At zero gap G' becomes

$$G=\frac{\pi^2A}{2e}\left(c_0+\frac{4\pi\epsilon^2}{k}-\frac{32\epsilon^2}{\pi k}\right)=\frac{\pi^2Ac}{2e}. \quad (33)$$

The effective elastic constant c' for a thickness-vibration resonator with gap is therefore

$$c'=c_0+c_1+c_2=c_0+4\pi\epsilon^2/k-32\epsilon^2e/\pi ke'. \quad (34)$$

This equation shows that the effective elastic constant c' is at zero gap slightly greater than the pure elastic constant c_0 and that the value increases with increasing gap. Herein lies the explanation of the change in the stiffness G' with gap referred to above. The gap effect is contained in the third term, which approaches zero for infinite gap.

The values of the piezo-capacitances C' and C in terms of the fundamental constants, from Eqs. (22), (23), (24), (32) and (33) are $C'=8\epsilon^2Ae/\pi^2e'^2c'$ and $C=8\epsilon^2A/\pi^2ec$.

For an X-cut quartz plate vibrating in the thickness mode the correction term c_1 has a value about 0.87 percent as large as c_0, while for zero gap c_2 is about 0.71 percent as large as c_0. Thus for zero gap the effective elastic constant c', for this cut, through the combined effects of c_1 and c_2, becomes about 0.16 percent greater than the pure elastic constant c_0. The natural resonator frequency, as the gap increases from zero to infinity, would therefore be expected to rise by about 0.3 percent (see §19).

The fact that G' in Eq. (32) consists of three terms suggests that C' in Eq. (23) may be regarded as equivalent to three capacitances in series. The values of the three are easily derived, but are of no importance in the present discussion.

We now consider briefly the effect of varying gap upon the curves in Fig. 3. For the same amount of strain, the curves for P and ρ remain unaltered, but the E curve, by Eq. (19), moves vertically downward as the gap increases, while the abscissas for maximum and minimum V shift correspondingly. Let the values of x corresponding to $E=0$ (maximum and minimum V) be denoted by $\pm x_m$. It is easily shown that, for gap w, $\cos \pi x_m/e=2e/\pi e'$ where $e'=e+kw$ as before. When $w=0$, $\cos \pi x_m/e=2/\pi$, whence $x_m=0.556e/2$, so that the E curve cuts the axis at points nearly midway between the center and the surfaces of the crystal. When $w=\infty$, $\cos \pi x_m/e=0$ and $x_m=\pm e/2$. The E curve then touches the points A and B without intersecting the axis at all, which corresponds to the vanishing of the third term in Eq. (34) at infinite gap.

§5. *Equivalence of the electrical and mechanical theories.* In the resonator theory given in §§2 to 4, the crystal with gap was treated as a unit, with a mechanical stiffness G' dependent on the gap. A necessary postulate, which was also implicit in the "electrical" theory, is that each surface of the crystal be equipotential; this condition is satisfied so long as the only wave-propagation is in the thickness direction.

It has already been stated that the values of R, L and C in Eq. (24), derived by the method of §3, are in agreement with Van Dyke's values, which are also used by Watanabe and others. In order to prove the complete equivalence of the electrical and mechanical theories, it only remains to show that Eqs. (23) and (24) are consistent with Eqs. (1) and (2). From Eqs. (23) and (24), $R'/R=L'/L=(e'/e)^2$. From the equations in §2 for C_1, C_2 and C_1' it is evident that this ratio is the same as $(C_1/C_1')^2=(1+C_1/C_2)^2$,

in agreement with Eq. (1). Agreement with Eq. (2) is found from Eqs. (23) and (24) together with (32) and (33). It thus becomes evident that, so far as thickness vibrations are concerned, polarization effects do not invalidate the assumption that the crystal can be treated as having fixed equivalent electrical constants R, L, C and C_1, with the gap capacitance C_2 in series.

(*b*) *Lengthwise vibrations*

§6. *Longitudinal vibrations in piezoelectric bars* have been treated theoretically and experimentally, by many authors (especially references 1, 2, 5, 8, 9, 11, 12, 13, 17, 18, 19). The present paper extends the theory to a consideration of surface charge and gap effects. Since the only experiments recorded here have to do with a quartz bar vibrating longitudinally in the direction of a mechanical axis, the field being parallel to an electrical axis (X-cut, Y-waves), the terminology applies only to this type, but the theory is equally applicable to any sort of piezoelectric bar of rectangular section excited by an electric field perpendicular to its length. On the experimental side most of the sources of error mentioned under thickness vibrations may be present.

The theory follows in general the same method as for thickness vibrations. (It is assumed that the bar is of sufficient breadth for edge effects to be neglected.) Using the same notation as before, we have[3,11,18] for a bar of dimensions e, l, b parallel to the x, y, z axes, respectively, and calling $bl=A$,

$$E_1=V/e_1, \quad M=\rho eA/2, \quad W=\pi^2\rho Qbe/2l,$$
$$G'=\pi^2bec'/2l.$$

As in the case of thickness vibrations, the logarithmic decrement is $\Delta=W/2fM$. The driving force impressed on the equivalent mass M is $F=F_0\cos\omega t$. The driving force involves the effective piezoelectric stress constant ϵ, which in the present case is not ϵ_{11} but δ_{11}/s_{11}, where s_{11} is an elastic compliance constant, and δ_{11} a piezoelectric strain constant. The proof of this lies in the fact that an electric field parallel to x excites the three piezoelectric stresses Y_y, X_z and Y_z, the last two of which, through the elastic cross constants (Poisson's ratio) make contributions to Y_y. From the fundamental piezoelectric and elastic relations[20] as applied to quartz, it follows that the total impressed stress causing longitudinal vibrations parallel to y is $(Y_y)_1=(\epsilon_{11}-\epsilon_{11}(s_{12}/s_{11})+\epsilon_{14}(s_{14}/s_{11}))E_1$, which is identically equal to $\delta_{11}E_1/s_{11}$ (reference 20, p. 817, Eq. (13)). This reasoning is correct only when the bar is so narrow that vibrations of the modes x_z and y_z have natural frequencies that are high in comparison with the y_y frequency; otherwise, X_z and Y_z would be met by counter stresses that would require modification of the equation for $(Y_y)_1$.

We may now write for the driving force, letting ϵ stand for δ_{11}/s_{11},

$$-F=2\epsilon beE_1=2\epsilon beV/e'=(2\epsilon beV_0/e')\cos\omega t.$$

The displacement at the end of the bar is $\xi=\xi_0\sin(\omega t-\theta)$, where (neglecting the sign)

$$\xi_0=F_0/\omega Z_c=2\epsilon beV_0/\omega e'Z_c,$$
$$Z_c^2=W^2+(\omega M-G'/\omega)^2.$$

The strain at distance y from the center is $y_y=(\pi\xi/l)\cos\pi y/l=Y_y/c'$, where Y_y is the stress at y and c' is the effective elastic coefficient. Since the only stress existing in the bar is Y_y, the polarization at y (parallel to the x axis) may best be expressed as $P(y)=\delta_{11}Y_y=-\delta_{11}c'y_y=-(\pi\delta_{11}c'\xi/l)\cos\pi y/l$, where δ_{11} is the piezoelectric strain-constant. Since, as will be seen, c' for a quartz bar is at all gap values very nearly equal to $1/s_{11}$, we may with negligible error write $\delta_{11}c'\approx\delta_{11}/s_{11}\equiv\epsilon$, as in the case of the driving stress. The polarization is distributed sinusoidally, being zero at the ends of the bar, with a maximum at the center, but it has no space variation parallel to the x axis. Hence it produces no space charge, but rather polarization surface charges $\sigma=\pm P$ at the boundaries. These charges give rise to a field component E_w and displacement D in the gap, which at any y has the value $E_w(y)=D(y)=4\pi P(y)e/e'$, an equation

[17] S. Namba and S. Matsumura, Researches of El. tech. Lab., Ministry of Communications, Tokyo, No. 248, April 1929.

[18] P. Vigoureux, *Quartz Resonators and Oscillators* (London, 1931).

[19] E. Giebe and E. Blechschmidt, Ann. d. Physik **18**, 457 (1933).

[20] W. Voigt, *Lehrbuch der Kristallphysik* (Leipzig, 1910) (or second edition, 1928), p. 901.

which may be generally proved for any uniformly polarized dielectric plate between parallel electrodes at zero potential. On substituting the value of $P(y)$ we find $D(y)=-(4\pi^2\epsilon e\xi/e'l)\cos \pi y/l$. $D(y)$ has the same sign as P; like P, it has a sinusoidal space variation parallel to the length of the bar, but is uniform in gap and crystal in the x direction. On the other hand, the field $E(y)$ in the dielectric caused by σ is of opposite sign to P and D. Its value may be shown to be

$$E(y)=-4\pi P(y)w/e'=(4\pi^2\epsilon w\xi/e'l)\cos \pi y/l. \quad (35)$$

We next find the expression for the current I in the resonator, analogous to Eqs. (15) and (21), the first term of which is unchanged. For the second term we need first the total electric flux φ over the surface A. This is obviously

$$\varphi=b\int_{-l/2}^{l/2} D\,dy=8\pi\epsilon be\xi/e'.$$

Hence

$$i'=\frac{1}{4\pi}\frac{d\varphi}{dt}=\frac{2\epsilon be}{e'}\frac{d\xi}{dt}=\frac{4\epsilon^2b^2e^2}{e'^2Z_c'}V_0\cos(\omega t-\theta)$$

$$=\frac{V_0}{Z'}\cos(\omega t-\theta),$$

where the equivalent electrical impedance is $Z'=\{R'^2+(\omega L'-1/\omega C')^2\}^{\frac{1}{2}}$. As in Eq. (22), we write $r'=e'^2/4\epsilon^2b^2e^2$, $r=1/4\epsilon^2b^2$ and have

$$R'=Wr', \quad L'=Mr', \quad C'=1/r'G' \quad (36)$$

and for zero gap,

$$R=Wr, \quad L=Mr, \quad C=1/rG. \quad (37)$$

As in the case of thickness vibrations, so also here $C_1=kA/4\pi e$, $C_1'=kA/4\pi e'$.

It remains to find G for zero gap and G' for gap w. Instead of the two stiffness terms G_1 and G_2 in Eq. (32) we now have only one, designated as G_1, since there is but one term in Eq. (35) for E. The reacting stress Y_y' due to the depolarizing field E, corresponding to X_1 and X_2, Eq. (26), is found from Eq. (35), using the same piezoelectric constant ϵ as in the case of the driving stress. At any value of y,

$$-Y_y'(y)=\epsilon E(y)=\frac{4\pi^2\epsilon^2w\xi}{e'l}\cos\frac{\pi y}{l}$$

$$=\frac{4\pi\epsilon^2w}{e'}y_y\equiv c_1y_1. \quad (38)$$

The "quasi-elastic constant" $c_1=4\pi\epsilon^2w/e'$ is always positive, hence it must be added to the pure elastic constant, which for a bar is Young's modulus. For a quartz bar perpendicular to the principal (z) axis this constant is $1/s_{11}$ (references 5, 8, 21, 22, 23, 24). The effective elastic constant with gap w is therefore

$$c'=c_0+c_1=\frac{1}{s_{11}}+\frac{4\pi\epsilon^2w}{e'}=\frac{1}{s_{11}}+\frac{4\pi\delta_{11}^2w}{e's_{11}^2}. \quad (39)$$

At zero gap this reduces to $c=c_0=1/s_{11}$, the pure elastic constant. As the gap approaches infinity, c' approaches the value $1/s_{11}+4\pi\delta_{11}^2/ks_{11}^2$ and the frequency increases correspondingly. The effective value of the compliance constant, which we will call s_{11}', is therefore for infinite gap $s_{11}'=s_{11}-4\pi\delta_{11}^2/k$, in agreement with Giebe and Scheibe,[5] whose deductions, reached by a different method, are based on the tacit assumption of infinite gap. Setting $s_{11}=12.95(10^{-13})$, $\delta_{11}=-6.9(10^{-8})$, $k=4.46$ (Table I), one finds that $4\pi\delta_{11}^2/k=0.13(10^{-13})$, which is approximately one percent of s_{11}.

The values of the piezo-capacitances C' and C in Eqs. (36) and (37) can now be given in detail. By the method described in §4, we find $C'=\pi^2bec'/2l$, $G=\pi^2be/2ls_{11}$, whence

$$C'=8\epsilon^2bel/\pi^2e'^2c', \quad C=8\epsilon^2bls_{11}/\pi^2e. \quad (40)$$

If the vibrating bar, when a gap w is present, were strictly equivalent to a bar with zero gap in series with a condenser $C_2=bl/4\pi w$, the values of R', L', C', R, L and C in Eqs. (36) and (37) should satisfy Eqs. (1) and (2). This is at once seen to be the case for the ratios R'/R and L'/L, but not for C'/C. Eq. (2) is easily converted into the form

$$C/C'=(e'^2/e^2)(1+eC/e'C_2), \quad (41)$$

[21] W. P. Mason, Bell Sys. Tech. J. **13**, 405 (1934).
[22] R. B. Wright and D. M. Stuart, Bur. Standards J. Research **7**, 519 (1931).
[23] I. Koga, Proc. I. R. E. **24**, 510 (1936).
[24] I. Koga, Proc. I. R. E. **24**, 532 (1936).

while from Eqs. (36) and (37) we obtain

$$\left(\frac{C}{C'}\right)=\frac{e'^2}{e^2}\left(1+\frac{\pi^3 weC}{ble'}\right)=\frac{e'^2}{e^2}\left(1+\frac{\pi^2}{8}\frac{eC}{e'C_2}\right). \quad (42)$$

The discrepancy lies in the fact that when the electric flux in the gap is sinusoidally distributed, so that the crystal surface is not equipotential, the simple equation for C_2, which is assumed in Eqs. (41) and (42), no longer holds. The discrepancy disappears at zero gap, since the crystal surfaces are then equipotential.

These considerations show that in the case of a bar driven by a transverse alternating electric field it is not permissible to treat the resonator as an $RLCC_1$ mesh in series with the capacitance of the gap, as in Fig. 1a. It is, however, correctly represented in terms of the electrical equivalents $R'L'C'C_1'$ given by Eqs. (36); or C' may be derived from Eq. (40) or (42). The dependence of frequency upon gap is given by Eqs. (45) and (47a).

§7. *Crystal bar metallically coated.* If the two faces of the bar that are normal to the electric field are lightly silvered, thereby causing them to remain equipotential even when there is a gap, the analysis employed in the last section shows that the only equivalent electrical constants to be altered are C and C'. This alteration comes about through the fact that Y_y' now has a *constant* value throughout the bar, namely the value given in Eq. (38) averaged from $-l/2$ to $l/2$. The corresponding quasi-elastic constant, which may be called c_2, is derived by the method used in deriving Eq. (29) and has the value $c_2=32\delta_{11}^2 w/\pi s_{11}^2 e'$. This takes the place of c_1 in Eq. (39), from which it differs by the factor $8/\pi^2$, indicating a slightly lower resonant frequency, when there is a gap. At infinite gap the difference amounts to about one-tenth percent. The effective elastic constant is $c'=c_0+c_2$, and this is the value to use in computing G' and C' for a silvered plate with gap. C_2 assumes at all gaps the simple form $C_2=bl/4\pi w$. In this case, and only then, can the resonator be regarded as equivalent to Fig. 1a, C_2 representing the geometrical capacitance of the gap.

In all the above expressions for capacitance it must, of course, be remembered that the formula for infinite parallel plates ceases to be even approximately correct when the gap length w approaches the crystal width b in value. Reliable experimental tests must, therefore, be confined to relatively short gaps.

II. Various Cuts and Their Fundamental Constants

List of cuts employed

§8. In Table I the first column indicates the cuts for which experimental data were obtained. "x" and "y" signify plates perpendicular to the x and y axes, respectively. The AC- and BT-cuts are those described by Lack, Willard and Fair;[25] similar investigations were published almost simultaneously by other writers.[26–29] For a right quartz crystal the last two cuts may be considered as obtained by rotating a Y-cut plate

[25] F. R. Lack, G. W. Willard and I. E. Fair, Bell Sys. Tech. J. **13**, 453 (1934).

[26] R. Bechmann, Naturwiss. **21**, 752 (1933); Hochfreq. tech. u. Elek. akus. **44**, 145 (1934).

[27] I. Koga and N. Takagi, J. Inst. Elec. Eng. of Japan **53**, 940, 1141 (1933).

[28] I. Koga, Rep. of Radio Res. in Japan **4**, 61 (1934); Doc. No. 33, Comm. I, U. R. S. I. Gen. Assembly, London 1934.

[29] H. Straubel, Physik. Zeits. **35**, 179 (1934); see also Zeits. f. tech. Physik **15**, 607 (1934).

Table I. *Data for various cuts.* For the values of c_0, see Table III. The magnitudes of the quasi-elastic constants c_1 and c_2, Eq. (34), may be derived from the last two columns. For the quasi-elastic constants of the bar, see §§6 and 7.

Cut	Type of Vibration	Type of Strain	k	ϵ	c_0	$\frac{4\pi e^2}{k}$	$\frac{32e^2}{\pi k}$
				$\times 10^4$		$\times 10^8$	$\times 10^8$
X	thickness compressional	x_x	4.42	$\epsilon_{11}=-5.1$	c_{11}	74	60
Y	thickness shear	x_y	4.42	$\epsilon_{11}=-5.1$	$c_{66}=\frac{1}{2}(c_{11}-c_{12})$	74	60
AC	" "	x_y'	4.46	$\epsilon_{26}'=-3.16$	c_{66}'	28	23
BT	" "	x_y'	4.53	$\epsilon_{26}'=-2.86$	c_{66}'	6	5
bar $\parallel y$	lengthwise compressional	y_y	4.46	$\delta_{11}/s_{11}=-5.33$	$1/s_{11}$	—	—

about the x axis through an angle θ, this angle being positive when the rotation is clockwise on sighting along the positive direction (Voigt's definition, reference 20, pp. 750, 859) of the x axis. For a left quartz the sign of θ is to be reversed. The value of this angle found by Lack, Willard and Fair for a right quartz is for the AC-cut 31°, and for the BT-cut, −49°.

In the third column of Table I is indicated the type of strain (and therefore of stress) for each cut. Primed symbols indicate rotated axes.

Elastic constants

§9. For thickness vibrations, the proper elastic constant for each cut, which in generalized form was denoted by c_0 in §4, is that one of the c's (in Voigt's notation) which expresses the stress-strain relation characteristic of the type of vibration.[10, 21] In quartz, the difference between the adiabatic and isothermal values is less than that between isothermal values as reported by different observers. The reason why c should be employed rather than the reciprocal of a compliance constant s is, that while there is but one strain, there is a system of lateral stresses (constraints) to which the absence of other strains is due. This statement is of course rigorously true only of infinite plates.

For lengthwise vibrations of a narrow bar parallel to the y axis, the expression for Young's modulus is $1/s_{11}$, as was stated in §6.

The specific form assumed by the generalized constant c_0 for each of the cuts discussed in §19 is indicated in the fourth column of Table I. Numerical values are given in §19. For the derivation of c_{66}' see reference 25, p. 463. The primes indicate oblique cuts with transformed axes.

In carrying out the final computations it was deemed wisest to derive the effective values c of the elastic constants from the measured frequencies, using the formula $c=4\rho f^2e^2$ (or $4\rho f^2l^2$ for the bar) where the density $\rho=2.65$. These values are shown in Table III for each crystal. From them, with the aid of Eqs. (34) and (39), the pure elastic constants c_0 have been calculated (see Table III). For comparison it may be noted that Voigt's values (adiabatic) for c_{11}, c_{66} and $1/s_{11}$ are, respectively, 8.54, 3.91 and 7.72, all times 10^{11} dynes/cm^2.

The dielectric constants

§10. Whenever the dielectric constant of a piezoelectric crystal is measured by the usual method of placing a plate of the material in an electric field, the observed value is always too great (reference 20, p. 917; reference 1, second citation, p. 749), owing to the deformation and consequent polarization caused by the electric field. The pure dielectric constant could be directly measured only if during the measurement the plate were kept unstrained, which is practically impossible.

On applying to Voigt's Eq. (287) (reference 20, p. 917) the subscripts for an X-cut in quartz, there results for the polarization produced by a field E, $P_1=(\eta_{11}+\epsilon_{11}\delta_{11}+\epsilon_{12}\delta_{12}+\epsilon_{14}\delta_{14})E_1$, for static conditions with the plate devoid of external stresses. η_{11} is the dielectric susceptibility parallel to the x axis. With thickness vibrations in an infinite plate each unit of volume is subject to external stresses due to the lateral constraints which neutralize the last two terms. The strain corresponding to the second term, which is of the type x_x, is replaced by the vibrational strain from which the piezo-current i, Eq. (15), is found, so that the only pure dielectric polarization caused by the impressed field is $P_1=\eta_{11}E_1$, from which it follows that $k=1+4\pi\eta$, the value for an unstrained crystal. The best value of the observed dielectric constant of quartz perpepdicular to the optic axis (crystal free from constraints) is 4.5.[30] From Voigt's equation, and setting $\epsilon_{11}\delta_{11}+\epsilon_{12}\delta_{12}+\epsilon_{14}\delta_{14}=0.0068$, we have $4.5=1+4\pi\eta+4\pi(0.0068)$, whence $k=1+4\pi\eta=4.42$ for the unstrained crystal. Since the susceptibility η is the same in all directions perpendicular to the optic axis, it follows that $k=4.42$ is the proper value for both X- and Y-cut plates (Table I). In the case of the AC- and BT-cuts it is necessary to compute k from the observed values parallel and perpendicular to the optic axis, namely 4.6 and 4.5, respectively.[30] The results are recorded in Table I. The values of k in different directions are so nearly alike that refraction of electric lines at the surface of the quartz (when there is a gap) may be ignored.

In the case of lengthwise vibrations, the stresses corresponding to the terms $\epsilon_{11}\delta_{11}$ and

[30] R. B. Sosman, *The Properties of Silica* (New York, 1927), p. 515.

$\epsilon_{14}\delta_{14}$ are not neutralized by external constraints, whence it is found that the effective dielectric constant is 4.46.

Although these distinctions are too small to be easily noticeable in quartz, it seems worth while to call attention to them, since they may easily play a more important part in resonators employing other crystals.

Piezoelectric constants

§11. The values adopted for ϵ_{11} and δ_{11} are taken from the *International Critical Tables*, Vol. VI: $\epsilon_{11}=-5.1(10^4)$, $\delta_{11}=-6.9(10^{-8})$. The sign applies to left quartz; for right quartz it should be reversed. The distinction is, of course, of no importance in the present vibrational equations. For s_{11} in Table I, Voigt's value, with the adiabatic correction, is used: $s_{11}=12.95(10^{-13})$ cm²/dyne. The values of ϵ_{26}' for the *AC*- and *BT*-cuts were computed by Voigt's method (reference 20, p. 840), modifying his equations for rotation about the x axis.[31]

III. Graphical Treatment of the Resonator

Resonance circle diagram

§12. The relations between various parameters, as well as the contrast between the electrical and the mechanical theories, can best be understood by means of the resonance circle diagram, Fig. 4. The treatment previously described[32] will be employed, according to which the same diagram serves for both admittances and impedances. We shall first explain the construction of the diagram representing Fig. 1a, according to the electrical theory, and then interpret it in terms of the mechanical theory. When there is no gap, the circle is based on the electrical constants R, L and C, Fig. 1a, which were shown in Eqs. (24) to be proportional to the mechanical constants W, M and $1/G$. It therefore represents in electrical terms the state of vibration of the resonator. In order to adapt the diagram to both impedances and admittances, the two unit vectors (scale-values) s_y and s_z are introduced, representing, respectively, the

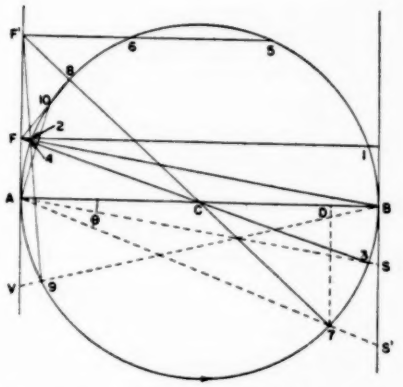

FIG. 4. Resonance circle diagram. Origin is at F′ when gap is present, approaching F as the gap diminishes to zero.

number of reciprocal ohms ("mhos"), and the number of ohms, per unit distance on the diagram. If $\rho_0=$AC is the radius of the circle in terms of unit distance, then $s_y\cdot 2\rho_0=1/R$, and the length of the line from A to any point on the circle, multiplied by s_y, represents to scale the admittance Y of the *RLC* branch at the frequency corresponding to that point. For example, at point 7, Fig. 4, the *RLC* admittance is $Y=s_y\cdot$A7, having components $g=s_y\cdot$AD and $b=s_y\cdot$D7.

From Eqs. (9), (13) and (24), it is evident that any line from A to a point on the circular locus, as for example A7, with proper choice of scale values (Table II), also represents the mechanical admittance $Y_c=s_c\cdot$A7, as well as the maximum velocity of motion, $v_0=s_v\cdot$A7. s_v is expressed in cm/sec. per unit of V per scale division. Velocity, mechanical admittance and equivalent electrical admittance, all have the same circular locus and, for any frequency, the same phase angle θ, defined by Eq. (12). Positive values of θ lie above the horizontal, indicating an inductive equivalent circuit for *RLC*.

From Eq. (13) it is seen that the amplitude of vibration ξ_0 has also very approximately a circular locus. The maximum amplitude does not come at the frequency corresponding to point B, however, but at a very slightly higher frequency, the angular velocity being $(G/M-W^2/2M^2)^{\frac{1}{2}}=(\omega_0^2-2\alpha^2)^{\frac{1}{2}}$, where ω_0 is the angular velocity at B and α is the damping constant (reference 12, p. 5). The scale value for ξ_0 is that for v_0 divided by ω.

[31] In the 1910 edition of Voigt the wrong sign occurs before the second parenthesis in the equation for ϵ_{26}', p. 841. This has been corrected in the 1928 edition.

[32] W. G. Cady, Proc. Am. Ac. **68**, 383 (1933).

The frequency distribution around the circle depends on R, L and C (not at all on C_1), and runs counterclockwise for admittances, as indicated by the arrow in Fig. 4, and clockwise for impedances. In the case of the admittance diagram for RLC the frequency is zero at A, increasing over the lower half of the circle to the resonance value f_0 at B, and finally reaching the value infinity at A.

The vertical line through B serves as a convenient frequency scale, the scale being very approximately linear over the resonance region (reference 33, p. 135; reference 32, p. 390). It is only necessary to prolong the line from A through the point on the circle for which the frequency f is desired until it meets the vertical line through B at some point S. Then to a close approximation $n=\sigma\cdot$BS, where $n=f-f_0$ and $\sigma=R/(8\pi\rho_0 L)$. BS is positive for points above the AB axis. As an illustration, the construction has been carried out in Fig. 4 for point 3. For points on the left half of the circle the distance BS becomes inconveniently large. In this case an alternative formula may be used (reference 32, p. 391): $n=\sigma'/$AV, where $\sigma'=\rho_0 R/2\pi L$ and V is the point on the vertical axis through A where the prolongation of the line from B through the point on the circle meets this axis. This case is also illustrated in Fig. 4 for point 9, V being the corresponding point on the frequency scale, and $n=\sigma'/$AV being the frequency-difference f_B-f_9. The AV scale is not linear, and like the BS scale it is accurate only over the resonance region. Because of the very low decrement of the resonator, all of the circle except a small region close to A corresponds to frequencies differing but little from f_0. f_0 is that frequency for which the reactance of the RLC branch vanishes ($4\pi^2 f_0^2=1/LC$); it is therefore the frequency of maximum velocity of motion under constant driving force (Eq. 13).

The $RLCC_1$ mesh

§13. In order to represent the admittance Y_1', of the $RLCC_1$ mesh at the frequency corresponding to any point P on the circle, we lay off AF$=-\omega C_1/s_y$ along the vertical axis. The upward direction is chosen in order that, when F is taken as the origin of vectors, capacitive values will come below the horizontal. The frequency varies so little over the resonance range that the points F and F′ may be regarded as fixed. The vector sum FP of FA and AP represents Y_1', P being any point on the circle. For example, at frequency f_0, P coincides with B and $s_y\cdot$FB$=Y_1'$; this shows that at the frequency for maximum velocity the electrical admittance of the crystal is slightly capacitive. At all frequencies above the horizontal line through F the crystal admittance is inductive. At points 1 and 2 the crystal behaves as a pure resistance. The admittance at 1 is large, and the frequency is very slightly above f_0. At 2, F2 is small and the condition is that of parallel resonance; the admittance F2 is for most resonators much smaller, even, than is shown in Fig. 4. This is because the distance AF has been greatly exaggerated for clearness: for a good resonator the ratio AF : AB$=\omega C_1 R$ is of the order 1 : 100. The frequencies for maximum and minimum admittance Y_m' and Y_n' fall at the points 3 and 4 (vector from F through C). At 4 is the condition of "antiresonance." The analytic expressions for the various vectors are cumbersome and need not be given. Dye[2] gives an extensive analytic treatment, while the general equation for the admittance of a resonator with gap has been derived by Usui.[34]

Crystal with gap

§14. The method of deriving an admittance diagram for $R'L'C'C_1'$, Fig. 1b, analogous to that for $RLCC_1$, consists first in inverting the latter, which may for brevity be called the s_y diagram, into an impedance, or s_z, diagram, keeping F as origin. The origin is next shifted to F′, the location of which is determined by the equation $s_z\cdot$AF′$=-1/\omega C_1'$ or $s_z\cdot$FF′$=-1/\omega C_2$, where s_z, the impedance scale value, is $1/s_y$(AF)^2 (reference 32, pp. 389, 396). We thus obtain the impedance diagram for $RLCC_1C_2$. One more inversion, this time with respect to F′, is now performed, giving the desired $R'L'C'C_1'$ admittance diagram (the s_y' diagram). F′ becomes the origin of admittance vectors, and s_y'AF′$=-\omega C_1'$. The value of R' is expressed by an equation analogous to that for the s_y diagram:

[33] E. Mallett, *Telegraphy and Telephony* (London, 1929).

[34] R. Usui, J. Inst. Elec. Eng. of Japan **54**, 201 (1934) (in Japanese; summary in English, ibid., p. 21).

TABLE II. *Resonance diagram notation.*

NETWORK	ORIGIN	VECTOR	ELECTRICAL	SCALE VALUES MECHAN. ADMITTANCE	VELOCITY
RLC	A	Y	$s_y=1/2\rho_0 R$	$s_c=rs_y$	$s_v=\dfrac{2\epsilon A}{e}s_c$
$RLCC_1$	F	Y_1'	"	$=\dfrac{e^2}{8\epsilon^2\rho_0 A^2 R}$	$=\dfrac{e}{4\epsilon\rho_0 A R}$
$RLCC_1$	F	Z_1'	$s_z=1/(\mathrm{AF})^2 s_y$		
$RLCC_1C_2$	F′	Z_2'	"		
$RLCC_1C_2$	F′	Y_2'	$s_y'=1/(\mathrm{AF}')^2 s_z$	$s_c'=r's_y'$	$s_v'=\dfrac{2\epsilon A}{e'}s_c'$
$RLCC_1C_2C_3$	F_3'	Y_3'	"	$=\dfrac{e'^2}{8\epsilon^2\rho_0 A^2 R'}$	$=\dfrac{e'}{4\epsilon\rho_0 A R'}$
$RLCC_1C_2C_3$	F_3'	Z_3'	$s_z'=1/(\mathrm{AF}_3')^2 s_y$		

$s_y'\cdot 2\rho_0=1/R'$. The quantities involved are summarized in Table II.

Consider, for example, point 3, Fig. 4, at a frequency f_3 slightly less than f_0. We have $Y=s_y\cdot$A3, $Y_1'=s_y\cdot$F3. According to the principle of inversion, Z_1', the reciprocal of Y_1', is obtained from 4, the point inverse to 3 with respect to F, that is, $Z_1'=s_z\cdot$F4. The vector sum of F′F and F4 is F′4, or $Z_2'=s_z\cdot$F′4. By inverting 4 with respect to F′ we obtain point 9, from which the admittance, at the same frequency, of the entire network $RLCC_1C_2$, may be found: $Y_2'=s_y'\cdot$F′9.

The remarks that were made concerning points 1, 2, 3, 4 and 9 in §13 hold, when there is a gap, with respect to points 5, 6, 7, 8 and 10. If the gap is so great that AF′>AC, the reactance of the resonator is capacitive at all frequencies.

The circle diagram with F′ as origin thus represents the performance of the $R'L'C'C_1'$ network, Fig. 1b, and from Eqs. (23) it is evident that it represents also the state of mechanical vibration, just as was the case with zero gap. In particular, the frequency at B, which may be called f_0', is that at which the velocity v', and also the piezo-current i', is a maximum. Although it is not recognizable as a critical frequency by direct electrical observation, still f_0' is the resonant frequency that is most accurately characteristic of the piezoelectric behavior of the resonator, and as such is of fundamental importance. Being practically identical with the frequency of maximum amplitude ξ_0, it is the frequency observed in experiments using the interferometer or microscope. The greater the gap, the more is the value of f_0' in excess of f_0, the value for zero gap. This difference, according to the mechanical theory, is due to the dependence of the stiffness C', Eqs. (14) and (32), upon the gap. It is this recognition of the variation of the effective mechanical stiffness with gap, rather than the explicit use of the gap capacitance, that distinguishes the mechanical from the electrical theory. The advantage of the mechanical theory lies in the better description that it gives of the physical phenomena, as well as in the greater ease with which the vibrational state may be determined at any frequency, and therefrom the potential difference across the crystal and the danger of breakage (§15).

As the gap diminishes, F′ approaches F, and the resonator with zero gap becomes a special limiting case. Since the R'/L' ratio, and hence the decrement, are independent of the gap, it follows that the same frequency scale value σ (§13) holds at all gaps.[35] The quantities dependent on the gap are the position of the origin F′, the admittance scale value s_y, the frequency f_0' at B, and the distribution of frequencies around the circle. With a given gap, if a point on the circle is experimentally determined at a frequency f, the frequency f_0' may be found immediately by graphical construction, as was illustrated for points 3 and 9, Fig. 4, in §13. By performing two obvious in-

[35] Watanabe (reference 3, second citation, p. 710), finds experimentally an increase in decrement at very small gaps, due apparently to air friction.

versions with respect to F′ and F, it is easy to locate on the s_y circle the frequency f_0' at point B when there is a gap, or indeed the frequency at any point whatever on the s_y' circle. If the frequency f_m' for maximum admittance with gap has been observed (point 7), the graphical method shows at a stroke (by drawing F8) that the same frequency comes at point 10 on the s_y circle, which, as it depends on the fundamental constants, may be regarded as the fiducial circle. In general, the greater the gap, the more are the frequency values shifted *clockwise* around the circle.

Phase diagram

§15. The relative phases and magnitudes of the various periodic quantities involved in the resonator are shown in Fig. 5. As may easily be verified, they are derived from Fig. 4, for the frequency at point 7 on the admittance diagram with gap, origin at F′. For example, since F′7 represents the total admittance Y_2', it is evident that the total current I (Fig. 1) leads V by the angle 6F′8. The various vectors may be regarded as either maximum or r.m.s. values.

It is necessary first to explain the voltages V_c and V_ξ. V_ξ is the component of potential difference between the crystal surfaces (Fig. 3) due to the state of strain, on the assumption of zero p.d. between electrodes. It is therefore equal and opposite to the corresponding drop across the gap, which by Eq. (20) is $8\pi\epsilon\xi w/e'$. V_c is the actual p.d. between the crystal surfaces and is, therefore, the vector sum of V_ξ and V_1, as shown in Fig. 5, where $V_1 = eV/e_1$ is the primary voltage impressed on the crystal (Fig. 2). A general equation for V_c in terms of equivalent electrical constants is easily derived from the expression above for V_ξ, with the aid of Eqs. (4), (9) and (11):

$$V_c = V_0\left\{\frac{4\pi w Y'}{\omega A}\sin(\omega t-\theta)+\frac{e}{e_1}\cos\omega t\right\}.$$

The phase angles, derived from Fig. 4, are as follows, the notation "i_1' : $V=90°$" signifying that i_1' leads V by 90°, etc.: I : $V = \angle 6F'8$; I : $V_2 = 90°$; i_1' : $V = 90°$; i' : $V = \angle BA7$; V_c : I $= \angle 8F1$; V_c : i and V_c : $v = \angle BA10$; v : $\xi = 90°$; V_c : $\xi = 180°$; i_1 : $V_c = 90°$.

Fig. 5 shows the current components for both Fig. 1a and b. Thus I is the resultant of i and i_1 and also of i' and i_1'.

According to the *mechanical theory*, V_1 is the driving voltage at point 7, Fig. 4, and ξ, V_ξ and V_c are large because of approximate mechanical resonance, v being nearly in phase with V. According to the *electrical theory*, the crystal-gap combination is nearly in series resonance, the crystal reactance being strongly inductive, as is shown by the angle 10AB, Fig. 4. Point 10 is found by inverting 7 into 8 with respect to F′, then inverting 8 into 10 with respect to F; it is the point on the *RLC* admittance circle at which the frequency is the same as at 7 on the $R'L'C'C_1'$ admittance circle. Thus according to the *electrical* theory the crystal itself is far from resonance, but the amplitude is large because V_c, which is now regarded as the driving voltage, is large. This is in striking contrast with the *mechanical* theory, which says that the drop across the crystal is great *because the amplitude of vibration is large;* we have an apparent interchange of cause and effect! The reason lies in the fact that the mechanical theory regards the effective stiffness as dependent on the gap, as has already been explained. The relations would appear still more striking if it were feasible to draw vector diagrams for a normal crystal, in which the ratio $\omega C_1 : 1/R$ and hence AF : AB is of the order 1 : 100 or less.

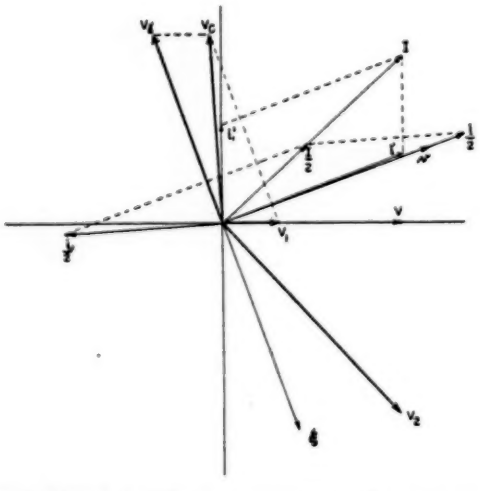

FIG. 5. Phase diagram for resonator with gap, based on Fig. 4. To save space, the vectors i and i_1 are drawn to half scale.

The production of very large voltages across the gap when the resonator is in the state of optimum gap resonance has been discussed by Dye[2] and the author.[32]

IV. Equations for Change in Frequency with Gap

Derivation of coefficient U

§16. Since the frequency of greatest theoretical importance is f_0' (§14), an equation will first be derived for $\Delta f = f_0' - f_0$, where f_0 (§12) is the limiting value of f_0' at zero gap. From the definitions of f_0 and f_0', and the relation $4e^2 f_0'^2 = c'/\rho$,

$$f_0'^2 - f_0^2 = (1/4e^2\rho)(c'-c) \approx 2f_0\Delta f. \qquad (43)$$

For thickness vibrations, from Eqs. (33), (34) and (43), it is easily found that

$$\Delta f/f_0 = (16\epsilon^2/\pi kc)(1 - e/e'),$$

or, remembering that $e' = e + kw$,

$$\Delta f/f_0 = 16\epsilon^2 w/\pi c e' \qquad (44)$$

where c is the value of c' at zero gap. In the limit, when $w = \infty$, this becomes $16\epsilon^2/\pi ck$.

For lengthwise vibrations, when the surfaces of the bar are not made equipotential by a metallic deposit, it is found by the above procedure, using Eqs. (36), (37), (39) and (40), that

$$\frac{\Delta f}{f_0} = \frac{2\pi\epsilon^2}{c_0}\frac{w}{e'} \approx 2\pi\delta_{11}^2 c_0 \frac{w}{e'}. \qquad (45)$$

An equation of the same form as (44) is found in the case of lengthwise vibrations when the surfaces of the bar are made *conductive*. The same equations are employed as in the derivation of Eq. (45), only in this case the expression for c_2 given in §7 takes the place of that for c_1 in Eq. (39). There results the equation

$$\frac{\Delta f}{f_0} = \frac{16\epsilon^2}{\pi c_0}\frac{w}{e'} = \frac{16\delta_{11}^2}{\pi s_{11}^2 c_0}\frac{w}{e'} \approx \frac{16\delta_{11}^2 c_0}{\pi}\frac{w}{e'}. \qquad (46)$$

This expression is smaller than that in Eq. (45) by the factor $8/\pi^2$.

The last three equations may be written in the general form $\Delta f/f_0 = Uw/e'$, the coefficient U in each case being a function of piezoelectric and elastic constants alone. It was the object of the experiments to compare this theoretical with the observed value of U.

When the crystal surfaces are equipotential, the effect of gap on frequency can also be expressed in terms of the gap capacitance C_2 (reference 2, p. 424; reference 18, p. 51). Thus from Eq. (44) we find for thickness vibrations, with the aid of Eqs. (24) and (33), together with the equation $w/e' = C_1/k(C_1+C_2)$,

$$\Delta f/f_0 = \tfrac{1}{2}C/(C_1+C_2). \qquad (47)$$

For infinite gap this becomes $C/2C_1$.

The same equation can similarly be derived for lengthwise vibrations (crystal silvered) from Eq. (46). In the case of lengthwise vibrations, when the bar is not metallically coated, it is found from Eq. (45) that

$$\Delta f/f_0 = (\pi^2/8)\cdot\tfrac{1}{2}\cdot C/(C_1+C_2). \qquad (47a)$$

The piezo-capacitance C can be measured electrically without reference to ϵ or c.[2, 3, 18] When this is done, Eq. (47) can be made to serve as a check on Eqs. (44), (45) and (46), and indeed it becomes a means of determining the piezoelectric coefficient ϵ at high frequency. No such observations were made with the crystals discussed in the present paper.

The theoretical relative change in frequency $\Delta f/f_0$, as the gap increases from zero to infinity, is easily found from the equations above by substituting for w/e' its limiting value $1/k$. It is approximately for the Y-cut 7.2; BT-cut 1.3; AC-cut 3.9; X-cut, thickness vibrations, 3.39; X-cut bar, unsilvered 5.1, silvered 4.2, all multiplied by 10^{-3}. The values of $1/k$ for the above cuts (see Table I) are, respectively, 0.226, 0.221, 0.224, 0.226, 0.224 and 0.224.

V. Observations and Results[36]

Apparatus

§17. With all thickness-vibration crystals a variable-frequency oscillator, the frequency of which could be controlled and read to one part

[36] The experimental work was carried out by Mr. John F. Müller. The writer wishes to express his thanks to the Bell Telephone Laboratories for the loan of certain crystals and for other courtesies.

in a million, was connected to the points a, b in Fig. 6, so that the resonator was excited by the voltage drop across the resistance R_0 of 600 ohms. Harmonic frequencies were removed by filters. For each observation the voltage was kept constant while the frequency f_m' was recorded at which the galvanometer G connected to a thermoelement indicated maximum current, (usually less than 0.5 ma), and hence maximum admittance of the $RLCC_1C_2C_3R_4$ network. The heater resistance R_4 had a value of 500 ohms. C_3 represents the stray capacitance of lead wires (Table III). Each crystal was carefully ground to uniform thickness and lay upon the lower electrode in a special mounting. The gap was regulated by a micrometer screw attached to the upper electrode. The faces of crystal X 1 were plane-parallel to within 4 microns, the other thickness-vibration crystals to within 1 micron. Tests with polarized light revealed no traces of twinning.

For crystal Q 30 (lengthwise vibrations) a different oscillator was used, and the difference $\Delta f_m'$ between the frequency at each gap and that at the smallest gap was observed. The same measuring circuit, Fig. 6, was used. This crystal rested horizontally upon the flat end of a round brass rod 1.5 mm in diameter which extended upward through the center of the lower electrode for a very short distance. It was clamped in position by a second brass rod 0.8 mm in diameter extending downward through the center of the upper electrode. The gap was varied by means of a micrometer screw which controlled the upper electrode. Only the fundamental lengthwise compressional mode was observed. Previous tests by dust-patterns had shown this to be the only perceptible mode. The resonant frequency, 66,500 cycles per second, was not appreciably altered by silvering. The designations Q 30 and Q 30s in Table III refer to this crystal in the unsilvered and silvered conditions, respectively.

In all cases the electrode faces were identical in size with those of the crystal. All the upper electrodes were made accurately plane, as were also the lower electrodes of crystals X 1 and Q 30. The lower electrodes of the remaining crystals were slightly concave, to a depth of not over 0.025 mm, in order that the central portions might be free to vibrate. Every precaution was taken to minimize stray capacitance. Approximate values of the equivalent resistances R had previously been determined (Table III). Values of L were computed from Eqs. (14) and (24).

Derivation of Δf from observed frequencies

§18. Because of the presence of C_3 and R_4 the observed frequency f_m' is not quite the same as f_0' in Eq. (43). If the resistance R_4 is negligible, f_0' is best derived from f_m' graphically, except with small gaps, when approximate formulas may be used. The graphical method is indicated in Fig. 7, in which, as in Fig. 4, F is the origin of vectors for the $RLCC_1$ mesh (zero gap), F_3 that for $RLCC_1C_3$ (zero gap, but including the stray capacitance C_3) and F′ the origin for the $RLCC_1C_2$ network, or its equivalent $R'L'C'C_1'$,

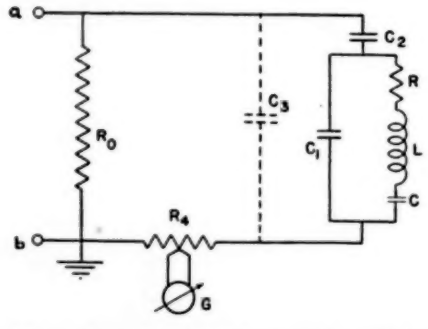

FIG. 6. Measuring circuit with resonator and thermoelement.

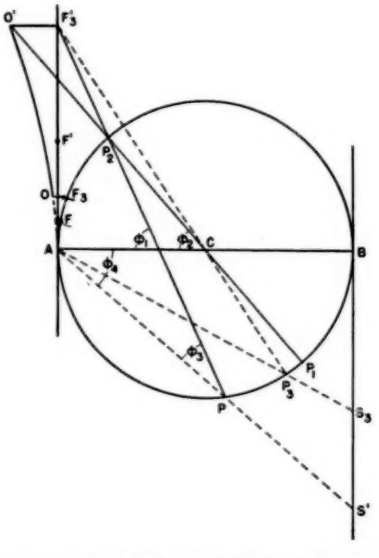

FIG. 7. Circle diagram for reduction of frequency observations.

Fig. 1. Since C_3 is in parallel with C_1', the origin for $R'L'C'C_1'C_3$ is at F_3', where $s_y' \cdot F'F_3' = -\omega C_3$ and

$$s_y' \cdot AF_3' = -\omega(C_1' + C_3). \quad (48)$$

Similarly, the point F_3 is determined by the equation

$$s_y \cdot AF_3 = -\omega(C_1 + C_3). \quad (49)$$

At the frequency corresponding to any point P on the s_y' circle, the admittance and impedance for $RLCC_1C_2C_3$ are, respectively, $Y_3' = s_y' \cdot F_3'P$ and $Z_3' = s_z' \cdot F_3'P_2$, P_2 being the point inverse to P with respect to F_3'.

If there is *no series resistance* R_4 to consider, the frequency f_m' for maximum admittance falls at point P_3, Fig. 7, whence $f_0' = f_m' + \sigma \cdot BS_3$ (§14), f_0' being the frequency at B. For zero gap (origin at F_3), the corresponding equation is $f_0 = f_m + \sigma \cdot BS_0$ where S_0 is the limiting position assumed by S_3 when the gap is zero.

The following expression, based on Fig. 7, makes it possible, when R_4 is negligible, to find BS_3/ρ_0 and BS_0/ρ_0 without actually performing the graphical construction: $BS_3/\rho_0 = \tan(BAS_3) = 2 \tan\{\frac{1}{2} \tan^{-1}(AF_3'/\rho_0)\}$. For each gap, including zero gap, AF_3' is to be found from Eq. (48).

When, as in the present case, the *series resistance* R_4 is large enough to have an appreciable effect on the resonance frequency, the graphical method offers a great advantage over the laborious algebraic process. The first step consists in inverting to the impedance diagram for $R'L'C'C_1'C_3$, the scale value being s_z', from Table II. This quantity, like s_y', has a different value for each gap. For any gap, when F_3', Fig. 7, has been located, the distance $O'F_3'$ is laid off horizontally to the left, by making $s_z' \cdot O'F_3' = R_4$, or (see Eq. (48) and Table II)

$$O'F_3' = -\omega R_4(C_1' + C_3)AF_3'. \quad (50)$$

O′ is then the origin of vectors for the entire circuit, including R_4. The locus of O′, as the gap varies, can be shown to be a parabola passing through A. The curve is most easily drawn by calculating $O'F_3'$ for two or three assumed values of w. At zero gap, $O'F_3'$ becomes OF_3.

When, for any gap, F_3' and O′ have been located, the line $O'P_1$ drawn through C represents the maximum admittance Y_m' of the entire circuit, and its inverse, $O'P_2$, represents the minimum impedance at the observed frequency f_m', since $s_z' \cdot O'P_2 = Z_n'$. The impedance, at this frequency, of the $RLCC_1C_2C_3$ network is $s_z' \cdot F_3'P_2$ and the admittance is $s_y' \cdot F_3'P$. From Fig. 7 it is seen that the frequency at P (which includes the effect of R_4) is lower than that at P_1, the point for maximum admittance when R_4 is negligibly small. The value of f_0' (§16) when R_4 is present is

$$f_0' = f_m' + \sigma \cdot BS', \quad (51)$$

where as before $\sigma = R/8\pi\rho_0 L$. At zero gap, the same procedure is followed for finding $f_0 = f_m + \sigma \cdot BS$, using O and F_3 in place of O′ and F_3'. Since AF_3, and also, for small gaps, AF_3', is usually small in comparison with the radius ρ_0, it is best at this end of the range to use the geometrical relations indicated in the diagram merely as a means for calculating BS′ for each gap, including the zero value. The equation is

$$BS'/2\rho_0 = \tan\varphi_4 = \tan(\varphi_1 - \varphi_3) = \tan(\varphi_1 - \varphi_2/2). \quad (52)$$

The angles φ_1 and φ_2 are easily expressed in terms of known quantities. This method was pursued in deriving the frequency differences Δf, with the exception of those for larger gaps, when the graphical method became necessary.

Finally, from the equations given above, the value of Δf for each gap (§16) is expressed, from Eq. (51), as

$$\Delta f = f_0' - f_0 = (f_m' + \sigma \cdot BS') - (f_m + \sigma \cdot BS), \quad (53)$$

where f_m and BS are the limiting values at zero gap. In practice, since it was not feasible to make observations strictly at zero gap, the values of f_0' were plotted against w/e', whence f_0 was found by extrapolation.

The magnitude of the $\sigma \cdot BS'$ correction ranged from 3∼/sec. for crystal Q 30 to 151∼/sec. for X 1. If this correction had not been applied, the value of Δf would have been lower by about 16 percent for X 2, 6 percent for X 1, and for the remaining crystals from 1.3 to 0.15 percent.

Results of observations

§19. The results are shown in condensed form in Table III and Fig. 8. The "calculated" (theoretical) values of U are the coefficients of

TABLE III. *Crystals tested and experimental results.* The first three crystals are *Y*-cut, the next two are cut according to Lack, Willard and Fair (§8). *X* 1 and *X* 2 are *X*-cut plates, *Q* 30 an *X*-cut bar for lengthwise vibrations, *Q* 30*s* the same silvered on both sides. For the *BT* and *AC*-cuts the *x*, *y*, *z* dimensions should be primed. Crystals *Y* 3 and *X* 1 are circular. Line 4, effective elastic constant at zero gap, according to §9. Line 9, correction $f_m'-f'$, §18, in cycles per sec., for maximum gap used. Line 11, wave constant in meters elmg. wave-length per mm in direction of vibration. Line 14, observed *U* for very small gap and for maximum gap. Line 16, percent excess of calculated over observed *U*.

The average values of the pure elastic constants c_0 (see §9) are: *Y*-cut, 4.15; *X*-cut (thickness vibrations), 8.81; *BT*-cut, 6.92; *AC*-cut, 2.88; *X*-cut bar (lengthwise vibrations) 7.66, all times 10^{11} dyne/cm². For the bar, $s_{11}=1/7.66\ (10^{11})=1.30\ (10^{-12})$ cm²/dyne.

CRYSTAL	*Y* 1	*Y* 2	*Y* 3	*BT*	*AC*	*X* 1	*X* 2	*Q* 30	*Q* 30*s*
1. *x* (cm)	3.8	3.8	2.5	3.8	3.8	0.286	0.40	0.152	0.152
2. *y* (cm)	0.30	0.99	0.262	0.335	0.335	4.5	3.8	4.04	4.04
3. *z* (cm)	3.8	3.8	2.5	3.8	3.8	4.5	3.8	1.40	1.40
4. $c(10^{-11})$ (dyne/cm²)	4.086	4.349	4.047	6.917	2.890	8.670	8.979	7.662	7.662
5. *R* (ohms)	200	200	200	200	200	700	1000	2470	2470
6. *L* (hen)	0.216	7.65	0.423	3.01	0.777	0.170	0.509	46.8	46.8
7. C_1 ($\mu\mu f$)	18.7	5.7	7.3	17.2	17.0	21.7	14.1	13.2	13.2
8. C_2 ($\mu\mu f$)	8.0	8.0	8.0	8.0	8.0	8.0	8.0	6.5	6.5
9. Max. $(f_m'-f')$(~/sec.)	63	11	30	4	11	151	91	3	3
10. f_0 (~/sec.)	654,060	204,427	745,198	761,974	492,550	1,000,422	727,598	66,500	66,500
11. *m/mm*	153	148	154	118	182	105	103	112	112
12. Max. *w* (cm)	1.26	1.45	0.85	0.98	0.72	0.084	0.25	0.48	0.47
13. Max. $\Delta f/f_0(10^3)$	5.27	3.56	2.93	0.76	2.52	0.78	0.53	4.15	3.35
14. Obs. *U*	0.0268	0.0238	0.0278	0.0060	0.0170	0.00875	0.00318	0.0200	0.0158
	0.0268	0.0182	0.0139	0.0038	0.0125	0.00615	0.00318	0.0200	0.0158
15. Calc. *U*	0.0324	0.0305	0.0327	0.00594	0.0176	0.0153	0.0147	0.0229	0.0186
16. % excess *U*	17	22	15	− 1	3	43	78	13	15
	17	40	58	+36	29	60	78	13	15

w/e' in Eqs. (44), (45) and (46), taking ϵ from Table I and *c* from Table III. "Observed" values of *U* are the ratios of observed $\Delta f/f_0$ to w/e'. According to theory, *U* should have a constant value for each cut, represented by a straight line of constant slope through the origin in Fig. 8. This expectation is approximately realized with crystals *Y* 1, *X* 2 and *Q* 30, while the characteristic lines for the remainder show a more or less decided curvature, indicating a decrease in *U* with increasing gap. Nearly always the observed values of *U* are too small, especially with the *X*-cut thickness-vibration crystals *X* 1 and *X* 2. In all cases, with the exception of the bar *Q* 30, the original curves showed, over certain gap ranges, effects of coupling within the crystal, or of air resonance, or both. The air resonance effect was very pronounced with the *X*-cut plates, as would be expected. In Fig. 8 the detailed curve is shown for crystal *Y* 1, illustrating strong mechanical coupling within the crystal.

In constructing Fig. 8, smooth lines were drawn through the plotted points, to correct as far as possible for these effects. There is no obvious reason why the lines so drawn should not be characteristic of the primary mode. On the original diagrams these lines were extended until they cut the $\Delta f/f$ axis. In each case, from the position of the intercept the basic frequency, f_0, was determined, from which the corrected value of Δf was found. It is most unfortunate that observations could not be made with the gap actually equal to zero, since the process of extrapolation led to some uncertainty in the precise determination of f_0, and hence of Δf.

By continuing the characteristic lines in Fig. 8 until they meet the ordinates for infinite gap (abscissa value $1/k$), one can gain an idea of how far the greatest possible increase in frequency with gap for the various crystals would fall short of the theoretical values for the various cuts given at the end of §16. This has been done in Fig. 8 for crystal *Y* 1 (Point P).

The relatively small values of *U*, even at small gaps, may have been due to one or more of the following causes: too large an assumed value for the piezoelectric constant in the theoretical value of *U*; traces of twinning; and the fact that the plates were not of infinite lateral extent. This last consideration must have tended, at any given gap, to make the frequency less than that for an infinite plate, in three ways, as follows: *First* by allowing some lines of electric intensity

to turn back around the edges of the plate, thus reducing the depolarization; *second* by increasing the effective capacitance of the gap, which has the same electrical effect as a reduction in gap thickness. These two effects are negligible at zero gap, but they grow in importance as the gap increases, thus offering a partial, if not complete, explanation of the curvature of the characteristic lines. The fact that the observed curvatures bear no consistent relation to the dimensions of the crystal plates indicates that this explanation is not of itself sufficient. The *third* consequence of the finite dimensions of the crystal is that, as the edges of the plate are approached, the lateral constraints mentioned in §9 diminish, resulting in a diminution in stiffness and hence in the wave velocity. The effect is the same as if the thickness of the plate increased slightly to a maximum at the edges. The natural frequency is thereby lowered, and owing to phase differences between the central and outer portions, the rate of increase in frequency with gap may also be diminished.

One more possible cause of diminution in slope of the characteristic line with increasing gap may be mentioned. If over the entire gap range the primary vibration mode is coupled to a high overtone of a secondary mode, this latter mode also having a frequency dependent upon the gap, then the observed U would be expected to diminish with increasing gap. For, in the case of the overtone, there are upon each surface of the crystal closely adjacent regions of positive and negative electrification, and as the gap increases, lines of electric intensity tend more and more to pass in a lateral direction from one such region to its neighbors instead of producing a depolarizing field in the crystal. The effective stiffness for this mode, and hence its frequency, is thereby decreased. From coupling theory it follows that the observed coupled frequency is also slightly decreased. That is, the rate of increase of observed frequency with increasing gap is less than if the overtone were absent, and since the effect increases with increasing gap, the characteristic line must diminish in slope as the gap increases.

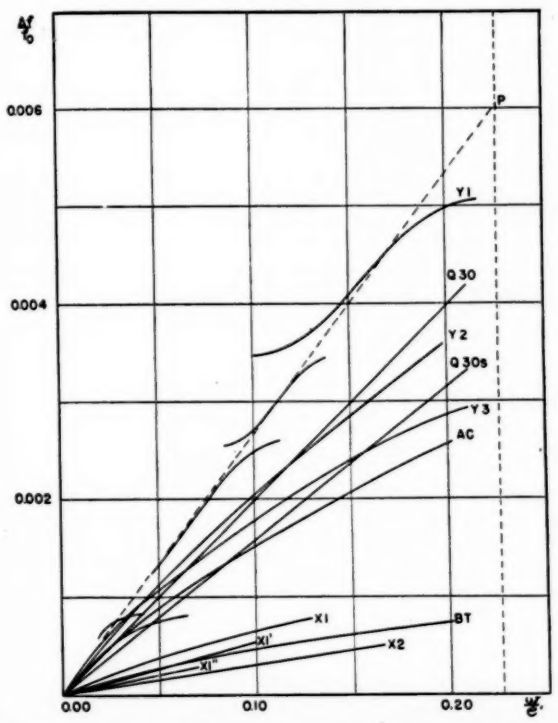

FIG. 8. Characteristic lines showing dependence of frequency upon gap for various crystals.

While these considerations suffice to account qualitatively for the observed anomalies in the gap effect, it remains impossible to assign specific reasons for individual cases. It is significant that the best agreement with theory, at least for small gaps, is found with the BT- and AC-cuts, both of which, especially the AC, are inclined at such an angle with the z axis as to reduce the coupling effects. Only comparatively weak evidences of coupling were, in fact, observed with these two cuts.

Of the X-cuts, X 2 had a practically constant but very low U at all gaps, over a wider range of gap than X 1. Both crystals had high resistances and required relatively high voltages for excitation. At small gaps, X 1 (a circular plate) had three prominent response frequencies, separated by a few hundred cycles. The results are represented by the characteristic lines X 1, X 1′, X 1″ in Fig. 8. Table III contains only the value of U for X 1, for very small and for maximum gaps, since this mode was the most pronounced of the three. On the whole, these results indicate that the almost universal practice of letting X-cut plates for thickness vibrations rest horizontally upon one electrode is not conducive to best operation.

A conclusion that may be drawn from all the observations is that a large increase in frequency

with gap, approximating the theoretical value, is a sign of a good resonator. It is hardly conceivable that any disturbing circumstance could make the observed U any *greater* than the theoretical value for the primary mode.

Effect of changing position of crystal in gap

§20. Brief mention should be made of the effect upon frequency of altering the *position of the crystal* between the electrodes. A test was made with crystal Q 30 (unsilvered) in which, while the total gap was left constant at 1.7 mm, the frequency was observed while the bar, always parallel to the electrodes, was moved by short stages from one side to the other. The frequency was a maximum with the bar in the central position, decreasing to a minimum as the bar was moved toward either electrode, and on still closer approach rising to a pronounced maximum, followed by a slight decrease just before contact with the electrode. The total variation was not over 5 cycles per sec., and played a quite insignificant part in determining the value of U. The maximum in frequency for the central position was found by Dye (reference 2, p. 450), and also still earlier by W. F. Powers in this laboratory. Both observers, however, recorded only a *decrease* in frequency as the crystal approached either electrode. It seems probable that this maximum is due to the finite width of the bar, by reason of which, as was explained above, some of the lines of electric intensity curve back around the edges; this effect, and the consequent diminution in frequency, may be expected to be slightly more pronounced when the crystal is close to one electrode. This view is strengthened by the fact that Dye's bar, which showed a much greater variation in frequency with position between the electrodes than Q 30, was relatively less than half as broad.

The rise in frequency of Q 30 to secondary maxima near the electrodes may have been an anomalous effect due to some peculiarity in the mounting. The voltage was too low to produce ionization. As the space between crystal and electrode becomes quite small, the periodic compression of the thin layer of air must increase the effective stiffness to a slight extent, but a simple calculation shows the effect to amount to a fraction of a cycle per second, and in fact the secondary maxima did not manifest themselves in the experiments in which the total gap was varied. Likewise negligible must be the increase in frequency due to the slight cooling of the vibrating quartz as it approaches an electrode. On the other hand, the rise in frequency may conceivably have been due to the approach to the first air-resonance point on the *wide* side of the gap. The decrease in frequency when the crystal was brought extremely close to one electrode may have been caused by increased air friction, as was reported by Watanabe (reference 3, second citation, p. 710).

These results point to the great importance, in work of high precision, of keeping the crystal in a fixed position with respect to the electrodes, and of mounting it in a vacuum.

Observations on Rochelle salt

§21. For comparison with the gap effect in quartz, a word may be added concerning a test made by the writer with *Rochelle salt*. The lengthwise vibration frequency at zero gap of a Y-cut bar 2.5 mm thick, measuring 21.3×5.9 mm in directions at 45° to the x and z axes, was roughly 56,800 cycles per sec. With a gap of 3.2 mm the frequency was 58,000, or about 2 percent greater. The effective value of Young's modulus was $c_0=1.03(10^{11})$ dyne/cm^2. On applying Eq. (46) and calling the dielectric constant $k=10$,[37] we find for the piezoelectric constant δ_{25} the value 134 (10^{-8}). This is in good agreement with the value 138 (10^{-8}) recorded by Valasek,[38] and somewhat less than Pockels' value[39] of 165 (10^{-8}). These observations indicate that if the elasticity and dielectric constant of a piezoelectric crystal are known, a rough approximation, at least, for the piezoelectric constant can be derived from gap observations.

Results of other observers

§22. Fig. 17 of Dye's paper[2] shows the dependence of frequency upon gap for thickness vibrations of an X-cut quartz plate $15.64\times16.40\times6.15$ mm. The writer has computed U from Dye's curve and found a mean value of 0.00536, about one-third of the theoretical value. Better

[37] H. Müller, Phys. Rev. **47**, 175 (1935).
[38] J. Valasek, Science **65**, 235 (1927).
[39] F. Pockels, Abh. d. kgl. Ges. d. Wiss. zu Göttingen **39**, 183 (1894).

agreement with theory is found from Fig. 30 in Vigoureux (reference 18, p. 68), for an X-cut quartz disk 9.43 mm diam., 0.58 mm thick. The theoretical value of U for this crystal is 0.0150, the value from the curve is 0.0137. Other records of frequency-gap observations have been published, for example, by Namba and Matsumura,[17] Koga[40] and Watanabe,[3] but the data are either insufficient or taken with the crystal in the generating circuit. Results obtained by the latter method are not characteristic of the resonator alone.

VI. Overtone Vibrations

Gap effect for overtones

§23. Since resonators have sometimes been employed with the crystal vibrating at an overtone frequency, it is of interest to examine the effect of varying gap on such frequencies. It is well known that, if f_1 is the fundamental frequency of thickness or lengthwise vibrations, a crystal will resonate at a frequency $f_n = nf_1$ approximately, where n is an odd integer. The writer has derived expressions for the equivalent constants for overtone vibrations, from which equations for the gap effect, analogous to Eq. (44), have been derived. Only the final results can be presented here.

With thickness vibrations it is found that $\Delta f_n/f_n = (1/n^2)(\Delta f_1/f_1)$, or in other words, the relative effect of gap on frequency is only $1/n^2$ as great for the overtone as for the fundamental. With lengthwise vibrations the value of $\Delta f_n/f_n$ for overtones turns out to be the same as for the fundamental. By using an even number of pairs of electrodes distributed uniformly along the length of the bar, *even* harmonics (approximately) of lengthwise vibrations can also be excited, in which case also the gap effect is the same as for the fundamental. These relations have not yet been tested experimentally.

[40] I. Koga, Proc. I. R. E. **18**, 1941 (1930).

Further Studies on the Mathematical Physics of Metabolizing Systems with Reference to Living Cells. II

N. RASHEVSKY, *University of Chicago*

(Received May 6, 1936)

A system of nonlinear differential equations, established in a previous paper, and describing the diffusion in a metabolizing system, which glycolizes and oxidizes sugar, is approximately integrated. With such values of the constants as are suggested by considerations of some biological systems, the average approximation obtained by this method is about three to five percent. The results are discussed and it is shown that they throw light on the variation of oxygen consumption of cells with varying oxygen concentration.

IN connection with a series of previous studies of the physics of the metabolizing systems,[1,2,3] we have discussed in a preceding paper[4] the system of differential equations which describes the consumption of sugar with subsequent glycolysis and oxidation. Using the same notations as before,[4] the system of equations is as follows:

$$\begin{aligned} &D_1\nabla^2 c_1 = ac_1; \quad \nabla^2 c_1' = 0, && \text{(a)}\\ &D_2\nabla^2 c_2 = -ac_1 + fc_2c_3; \quad \nabla^2 c_2' = 0, && \text{(b)}\\ &D_3\nabla^2 c_3 = 1.07fc_2c_3; \quad \nabla^2 c_3' = 0, && \text{(c)} \end{aligned} \tag{1}$$

with the boundary conditions,[4] for $r = r_0$:

$$\begin{aligned} D_1(dc_1/dr) &= h_1(c_1' - c_1), && \text{(a)}\\ D_1'(dc_1'/dr) &= D_1(dc_1/dr), && \text{(b)}\\ D_2(dc_2/dr) &= h_2(c_2' - c_2), && \text{(c)}\\ D_2'(dc_2'/dr) &= D_2(dc_2/dr), && \text{(d)}\\ D_3(dc_3/dr) &= h_3(c_3' - c_3), && \text{(e)}\\ D_3'(dc_3'/dr) &= D_3(dc_3/dr). && \text{(f)} \end{aligned} \tag{2}$$

We have discussed[4] the solution of this system for a very special limiting case, namely that of very large D's. We also have considered for that case the possible variations of the permeabilities h with the rates of metabolism. In the present paper we shall give a more general approximate solution of (1) and (2) for the case of spherical symmetry, considering however all h's and D's as constants.

Eqs. (1a) are independent on the others. For spherical symmetry, Eqs. (1a) reduce to

$$\begin{aligned} D_1[(d^2c_1/dr^2) + (2/r)(dc_1/dr)] &= ac_1, && \text{(a)}\\ d^2c_1'/dr^2 + (2/r)(dc_1'/dr) &= 0. && \text{(b)} \end{aligned} \tag{3}$$

A substitution

$$c_1 = u_1/r \quad \text{and} \quad c_1' = u_1'/r \tag{4}$$

transforms (3) into

$$d^2u_1/dr^2 = au_1/D_1; \quad d^2u_1'/dr^2 = 0. \tag{5}$$

Since $a > 0$[4], therefore the general integral of the first of Eq. (5) is

$$u_1 = A_1 \sinh (a/D_1)^{\frac{1}{2}}r + B_1 \cosh (a/D_1)^{\frac{1}{2}}r, \tag{6}$$

where A_1 and B_1 are constants of integration, and therefore

$$c_1 = A_1[\sinh (a/D_1)^{\frac{1}{2}}r]/r + B_1[\cosh (a/D_1)^{\frac{1}{2}}r]/r.$$

The requirement that c_1 remain finite for $r = 0$ makes $B_1 = 0$. Hence

$$c_1 = A[\sinh (a/D_1)^{\frac{1}{2}}r]/r. \tag{7}$$

The general integral of the second equation of (5) is

$$u_1' = A_1'r + B'$$

or

$$c_1' = A_1' + B_1'/r. \tag{8}$$

Since for $r = \infty$, $c_1' = c_{01}$, c_{01} denoting the external concentration at infinite distance, we have

$$c_1' = c_{01} + B_1'/r. \tag{9}$$

The remaining two constants A_1 and B_1' are determined by introducing (7) and (9) into (2a) and (2b). In this way after some elementary calculations the *exact* solution of (1a) and (2a) is obtained, which however is very cumbersome. A very good approximation leads however to a much simpler expression. We have, namely:

$$[\sinh (a/D_1)^{\frac{1}{2}}r]/r = 1 + ar^2/6D_1 + a^2r^4/120D_1^2 + \cdots. \tag{10}$$

[1] N. Rashevsky, Physics **5**, 374 (1934).
[2] N. Rashevsky, Physics **6**, 35 (1935).
[3] N. Rashevsky, Physics **6**, 117 (1935).
[4] N. Rashevsky, Physics **6**, 343 (1935).

With the range of values of a, r and D_1 which we have considered hitherto, and which are taken from biological considerations,[4] we find that the first two terms of expansion (10) constitute a very good approximation. Omission of the higher terms introduces an error of only one to five percent. We have therefore with a good approximation

$$c_1 = A_1(1 + ar^2/6D_1). \tag{11}$$

Hence
$$dc_1/dr = ar/3D_1 \tag{12}$$

while (9) gives

$$dc_1'/dr = -B_1'/r^2. \tag{13}$$

Substituting r_0 for r in (12) and (13) and introducing them into the (2b), we easily find

$$B_1' = -A_1 a r_0^3/3D_1'. \tag{14}$$

Introducing (14) into (9) and the latter together with (11) into (2a), we find after simple rearrangements

$$A_1 = c_{01}/[1 + (ar_0/3) \times (1/h_1 + r_0/D_1' + r_0/2D_1)] \tag{15}$$

(9), (11), (14) and (15) give us the desired approximate solution of (1a).

If we introduce (11) into (3a) we shall find that the left-hand side or $D_1\nabla^2 c_1$ becomes equal to $A_1 a$. Since however $D_1\nabla^2 c_1$ is equal at any point to the true rate of consumption of c_1 at that point, the introduction of the approximation (11) is physically equivalent to introducing, instead of the rate of reaction ac_1 per unit volume, which varies from point to point with c_1, an *average* constant rate of reaction $\bar{q}_1 = A_1 a$. We shall use this to solve approximately the other four Eqs. (1).

The first equations of (1b) and (1c), transformed to polar coordinates, give

$$D_2[d^2c_2/dr^2 + (2/r)(dc_2/dr)] = -ac_1 + fc_2c_3, \tag{16}$$

$$D_3[d^2c_3/dr^2 + (2/r)(dc_3/dr)] = 1.07fc_2c_3. \tag{17}$$

Solving (17) for fc_2c_3 and introducing it into (16), we have:

$$D_2[d^2c_2/dr^2 + (2/r)(dc_2/dr)] = -ac_1 + 0.94D_3[d^2c_3/dr^2 + (2/r)(dc_3/dr)]. \tag{18}$$

Introducing for c_1 the expression (11) and making the substitution:

$$c_2 = u_2/r; \quad c_3 = u_3/r, \tag{19}$$

we find

$$D_2(d^2u_2/dr^2) = 0.94D_3(d^2u_3/dr^2) - A_1a^2r^3/6D_1 - A_1ar. \tag{20}$$

Integrating this twice, we find

$$D_2u_2 = 0.94D_3u_3 - A_1ar^3/6 - A_1a^2r^5/120D_1 + \alpha r + \beta, \tag{21}$$

α and β being constants of integration.

Introducing again c_2 and c_3 according to (19), we have

$$D_2c_2 = 0.94D_3c_3 - A_1ar^2/6 - A_1a^2r^4/120D_1 + \alpha + \beta/r. \tag{22}$$

Since both c_2 and c_3 must remain finite for $r = 0$, we must have $\beta = 0$. Therefore (22) gives

$$c_2 = 0.94(D_3/D_2)c_3 - A_1ar^2/6D_2 - A_1a^2r^4/120D_1D_2 + \alpha/D_2. \tag{23}$$

If we knew c_3, we would know c_2, α being determined by the boundary conditions. c_3 is determined in its turn by (1c). Using the above outlined idea, we shall introduce instead of the variable rate of reaction for c_3, $1.07fc_2c_3$, an average constant rate $\bar{q}_3 = 1.07f\overline{c_2c_3}$, defined by

$$\bar{q}_3 = [1/(4/3)\pi r_0^3] \times 1.07f4\pi \int_0^{r_0} r^2c_2c_3\,dr. \tag{24}$$

If the rate of consumption of c_3 were constant and equal to $\bar{q}_3$, then the solution of (1c) with (2e) and (2f) would be[1]

$$c_3 = c_{03} - \bar{q}_3r_0/3h_3 - \bar{q}_3(r_0^2 - r^2)/6D_3 - \bar{q}_3r_0^2/3D_3', \tag{25}$$

$$c_3' = c_{03} - (\bar{q}_3r_0^3/3D_3')(1/r), \tag{26}$$

c_{03} being the external concentration of oxygen at infinite distance from the system. Hence these equations will express *approximately* the distribution of c_3 and c_3', if we can express $\bar{q}_3$ in terms of the other constants of the system (1) and (2).

To this end we introduce the abbreviations:

$$m = c_{03} - \bar{q}_3r_0/3h_3 - \bar{q}_3r_0^2/6D_3 - \bar{q}_3r_0^2/3D_3'; \quad n = \bar{q}_3/6D_3. \tag{27}$$

(25) thus becomes

$$c_3 = m + nr^2. \tag{28}$$

Introducing this into (23), we find

$$c_2 = 0.94(D_3/D_2)(m+nr^2) - A_1 a r^2/6D_2 - A_1 a^2 r^4/120 D_1 D_2 + \alpha/D_2. \tag{29}$$

Using again the previous values of the various constants,[4] we find that the term $A_1 a^2 r^4/120 D_1 D_2$ is small as compared with $A_1 a r^2/6D_2$ and we shall therefore omit it. The maximum error introduced by this is less than five percent. The average error is about two percent. The general integral of the second equation (1b) is again of the form:[1]

$$c_2' = c_{02} + (B_2'/r). \tag{30}$$

Differentiating (29) and (30) with respect to r, substituting r_0 for r and introducing into (2d), we find after simple rearrangements

$$B_2' = (A_1 a - 5.6 D_3 n) r_0^3/3D_2'. \tag{31}$$

Introducing this into (30), substituting then r_0 for r in (30) and in (29), and introducing both into (2c), we find after some rearrangements

$$\alpha = D_2 c_{02} - 0.94 D_3 m - (0.94 D_3 n - A_1 a/6) r_0^2 - (5.6 D_3 n - A_1 a)(r_0^2/D_2' + r_0/h_2) D_2/3. \tag{32}$$

We have thus expressed α in terms of m and n, or, on account of (27), in terms of the yet unknown quantity $\bar{q}_3$.

Substituting now (27) and (32) into (29), and omitting $A_1 a^2 r^4/120 D_1 D_2$, we find after elaborate but quite elementary rearrangements

$$c_2 = c_{02} + A_1 a(h_3 r_0^2 + D_3' r_0)/3h_2 D_2' + A_1 a(r_0^2 - r^2)/6D_2 - [0.3(h_3 r_0^2 + D_3' r_0)/h_2 D_2' + 0.16(r_0^2 - r^2)/D_2]\bar{q}_3. \tag{33}$$

On the other hand (25) can be written

$$c_3 = c_{03} - (2D_3 D_3' r_0 + 2D_3 h_3 r_0^2 + D_3' h_3 r_0^2 - h_3 D_3' r^2)\bar{q}_3/6D_3 D_3' h_3. \tag{34}$$

Or, introducing the notations

$$\gamma = A_1 a(h_3 r_0^2 + D_3' r_0)/3h_2 D_2' + A_1 a(r_0^2 - r^2)/6D_2,$$

$$\eta = 0.3(h_3 r_0^2 + D_3' r_0)/h_2 D_2' + 0.16(r_0^2 - r^2)/D_2, \tag{35}$$

$$\delta = (2D_3 D_3' r_0 + 2D_3 h_3 r_0^2 + D_3' h_3 r_0^2 - h_3 D_3' r^2)/6D_3 D_3' h_3,$$

we have

$$c_2 = c_{02} + \gamma - \eta\bar{q}_3; \quad c_3 = c_{03} - \delta\bar{q}_3. \tag{36}$$

Hence,

$$1.07 f c_2 c_3 = 1.07 f[c_{02}c_{03} + \gamma c_{03} - (\delta c_{02} + \gamma\delta + \eta c_{03})\bar{q}_3 + \eta\delta\bar{q}_3^2]. \tag{37}$$

The quantities γ, η and δ are quadratic functions of r. Hence the average $1.07 f\overline{c_2 c_3}$ is given by:

$$1.07 f\overline{c_2 c_3} = 1.07 f[c_{02}c_{03} + \bar{\gamma} c_{03} - (\bar{\delta} c_{02} + \overline{\gamma\delta} + \bar{\eta} c_{03})\bar{q}_3 + \overline{\eta\delta}\bar{q}_3^2] \tag{38}$$

with

$$\bar{\gamma} = [1/(4/3)\pi r_0^3] \times 4\pi \int_0^{r_0} r^2 \gamma\, dr \tag{39}$$

and similar expressions for $\bar{\eta}$ and $\bar{\delta}$.

From (35) $\bar{\gamma}$, $\bar{\eta}$ and $\bar{\delta}$ are very easily calculated, according to (39), and we find

$$\begin{aligned} \bar{\gamma} &= A_1 a(h_3 r_0^2 + D_3' r_0)/3h_2 D_2' + A_1 a r_0^2/15 D_2, \\ \bar{\eta} &= 0.3(h_3 r_0^2 + D_3' r_0)/h_2 D_2' + 0.06 r_0^2/D_2, \\ \bar{\delta} &= [2D_3 D_3' r_0 + 2D_3 h_3 r_0^2 + (2/5) h_3 D_3' r_0^2]/6D_3 D_3' h_3. \end{aligned} \tag{40}$$

But, according to (24), $1.07 f\overline{c_2 c_3}$ is itself equal to $\bar{q}_3$. Hence we have now an equation for the determination of $\bar{q}_3$, by making the right-hand side of (38) equal to $\bar{q}_3$

$$\bar{q}_3 = 1.07 f[c_{02}c_{03} - \bar{\gamma} c_{03} - (\bar{\delta} c_{02} + \overline{\gamma\delta} + \bar{\eta} c_{03})\bar{q}_3 + \overline{\eta\delta}\bar{q}_3^2]. \tag{41}$$

Eq. (40) expresses $\bar{\gamma}$, $\bar{\eta}$ and $\bar{\delta}$ in terms of the parameters of the differential equations. Using previous values for a, f, r_0, h_1, h_2, h_3 and taking[1, 3] $D \sim 10^{-7}$, we find that $\bar{\eta}$ and $\bar{\delta}$ are of the order of 1, while $\bar{\gamma}$ is of the order of 10^{-4}. On the other hand $\bar{q}_3$ is nothing else but the average rate of oxygen consumption, which is known for biological systems considered here to be of the order of magnitude of 10^{-4} g·cm^{-3}·min. With those values we find that the quadratic terms in (41) can be neglected and we find with good approximation

$$\bar{q}_3 = 1.07 f(c_{02} - \bar{\gamma}) c_{03}/[1 + 1.07 f(\bar{\delta} c_{02} + \overline{\delta\gamma} + \bar{\eta} c_{03})]. \tag{42}$$

The same result can of course be obtained by solving the quadratic equation (41) for $\bar{q}_3$, and then omitting small terms.

We now have a complete approximate solution of Eqs. (1) and (2). c_1 and c_1' are completely described by (11), (8), (14) and (15) in terms of $a, f, h_1, h_2, h_3, D_1, D_1', D_2, D_2', D_3, D_3'$ and r_0. In terms of the same parameters c_3 is described by (25), (42) and (40); while (23) and (32) give us an expression for c_2. c_2' and c_3' are given by (30), (31) and (26), (42), (40) correspondingly. With the approximation here used all internal concentrations are of the form $A+Br^2$ and all external of the form $E+G/r$, the coefficients A, B, E and G being expressed in terms of the 12 parameters a, f, h_1, etc.

A measure of the approximation thus obtained is given by the amounts by which γ, η and δ deviate from their corresponding averages $\bar{\gamma}$, $\bar{\eta}$ and $\bar{\delta}$. With the above discussed values for the physical constants used, a numerical estimation shows that the deviation of the extreme values from the averages is below three percent. The average error is therefore about one to two percent.

Because of a close interrelation between the three reactions described by (1), the concentration of any substance depends not only on the diffusion coefficient and permeability for this substance, but also on the diffusion coefficients and permeabilities of the other substances. A discussion of those rather complex relations from the point of view of biological applications will be given elsewhere. Here we shall discuss only one general property of our solution, which is also of great biological interest. We remark that the total rate of oxygen consumption Q_3 in the system is equal by definition to

$$Q_3=(4/3)\pi r_0^3\bar{q}_3. \tag{43}$$

Eq. (42) shows that if all other parameters are kept constant, but the external concentration of oxygen, c_{03}, is varied, $\bar{q}_3$ is zero for $c_{03}=0$, and with increasing c_{03} increases to an asymptotic value

$$(c_{02}-\bar{\gamma})/\eta. \tag{44}$$

Hence Q_3 will also increase from zero to an asymptotic constant value.

It has been observed[5] that in living cells the total oxygen consumption per cell is constant for high oxygen concentrations and drops to zero for low oxygen concentrations. An interpretation of this phenomenon has been attempted by R. W. Gerard[6] on the assumption of a strictly constant true rate of oxygen consumption, and ascribed to a limitation of the depth of penetration of oxygen due to a finite diffusion coefficient. A more general treatment has been given by N. Rashevsky,[7] so as to include effects of permeability. The assumption of a constant rate of reaction, independent of concentration, is however surely untenable for biological systems. The present study, free of this limitation, gives us a much more general insight into this phenomenon. In the present case it is due largely to the circumstance that the true rate of oxygen consumption is proportional to c_2c_3, that is, to both the concentration of oxygen and that of lactic acid. An increase of oxygen concentration results in an increased consumption both of oxygen *and of lactic acid*. This decreases c_2. The product c_2c_3 increases therefore less rapidly than c_3 alone, and tends to a constant value for infinite c_3, c_2 tending to zero.

This effect is found also when using the quadratic equation (41), which involves more calculations. The asymptotic value (44) for $\bar{q}_3$ is still in the range for which the quadratic term may be neglected.

Eq. (31) shows the interesting effect of the glycolytic constant a. If a is large enough, B_2' is positive, the concentration of lactic acid outside the system is decreasing with increasing r, which corresponds to a net production of lactic acid. This is the usual case. If a is very small, B_2' becomes negative. Lactic acid flows into the system. This could happen, when the breakdown of sugar is not rapid enough to supply sufficient lactic acid for oxidation. In the first case c_{02} may be made zero, without impairing the whole system of reactions. In the second case c_{02} must be kept finite. In order for the reactions to take place at all, there must be a supply of lactic acid.

[5] R. W. Gerard and P. S. Tang, J. Cell. Comp. Phys. **1**, 503 (1932); W. R. Amberson, Biol. Bull. **55**, 79 (1928); C. S. Shoup, J. Gen. Physiol. **13**, 27 (1929).

[6] R. W. Gerard, Biol. Bull. **60**, 245 (1931).

[7] N. Rashevsky, Protoplasma **20**, 125 (1933).